



Design and biological evaluation of substituted 5,7-dihydro-6 H -indolo[2,3- c]quinolin-6-one as novel selective Haspin inhibitors

Sreenivas Avula, Xudan Peng, Xingfen Lang, Micky Tortorella, Béatrice Josselin, Stéphane Bach, Stephane Bourg, Pascal Bonnet, Frédéric Buron, Sandrine Ruchaud, et al.

► To cite this version:

Sreenivas Avula, Xudan Peng, Xingfen Lang, Micky Tortorella, Béatrice Josselin, et al.. Design and biological evaluation of substituted 5,7-dihydro-6 H -indolo[2,3- c]quinolin-6-one as novel selective Haspin inhibitors. *Journal of Enzyme Inhibition and Medicinal Chemistry*, 2022, 37 (1), pp.1632-1650. 10.1080/14756366.2022.2082419 . hal-03818922

HAL Id: hal-03818922

<https://hal.science/hal-03818922>

Submitted on 28 Oct 2022

HAL is a multi-disciplinary open access archive for the deposit and dissemination of scientific research documents, whether they are published or not. The documents may come from teaching and research institutions in France or abroad, or from public or private research centers.

L'archive ouverte pluridisciplinaire **HAL**, est destinée au dépôt et à la diffusion de documents scientifiques de niveau recherche, publiés ou non, émanant des établissements d'enseignement et de recherche français ou étrangers, des laboratoires publics ou privés.



Design and biological evaluation of substituted 5,7-dihydro-6*H*-indolo[2,3-*c*]quinolin-6-one as novel selective Haspin inhibitors

Sreenivas Avula, Xudan Peng, Xingfen Lang, Micky Tortorella, Béatrice Josselin, Stéphane Bach, Stephane Bourg, Pascal Bonnet, Frédéric Buron, Sandrine Ruchaud, Sylvain Routier & Cleopatra Neagoie

To cite this article: Sreenivas Avula, Xudan Peng, Xingfen Lang, Micky Tortorella, Béatrice Josselin, Stéphane Bach, Stephane Bourg, Pascal Bonnet, Frédéric Buron, Sandrine Ruchaud, Sylvain Routier & Cleopatra Neagoie (2022) Design and biological evaluation of substituted 5,7-dihydro-6*H*-indolo[2,3-*c*]quinolin-6-one as novel selective Haspin inhibitors, Journal of Enzyme Inhibition and Medicinal Chemistry, 37:1, 1632-1650, DOI: [10.1080/14756366.2022.2082419](https://doi.org/10.1080/14756366.2022.2082419)

To link to this article: <https://doi.org/10.1080/14756366.2022.2082419>



© 2022 The Author(s). Published by Informa UK Limited, trading as Taylor & Francis Group.



[View supplementary material](#)



Published online: 07 Jun 2022.



[Submit your article to this journal](#)



Article views: 1026



[View related articles](#)



[View Crossmark data](#)

RESEARCH PAPER



Design and biological evaluation of substituted 5,7-dihydro-6H-indolo[2,3-c]quinolin-6-one as novel selective Haspin inhibitors

Sreenivas Avula^a, Xudan Peng^a, Xingfen Lang^a, Micky Tortorella^{a,e}, Béatrice Josselin^{b,c}, Stéphane Bach^{b,c}, Stéphane Bourg^d, Pascal Bonnet^d, Frédéric Buron^d, Sandrine Ruchaud^b, Sylvain Routier^d and Cleopatra Neagoie^{a,e}

^aGuangzhou Institute of Biomedicine and Health, Chinese Academy of Science, Guangzhou, China; ^bSorbonne Université/CNRS UMR8227, Roscoff cedex, France; ^cSorbonne Université/CNRS FR2424, Plateforme de criblage KISSf (Kinase Inhibitor Specialized Screening Facility), Roscoff cedex, France; ^dInstitut de Chimie Organique et Analytique, Université d'Orléans, UMR CNRS 7311, Orleans, France; ^eCentre for Regenerative Medicine and Health, Hong Kong Institute of Science and Innovation, Chinese Academy of Science, Hong Kong SAR, China

ABSTRACT

A library of substituted indolo[2,3-c]quinolone-6-ones was developed as simplified Lamellarin isosters. Synthesis was achieved from indole after a four-step pathway sequence involving iodination, a Suzuki-Miyaura cross-coupling reaction, and a reduction/lactamization sequence. The inhibitory activity of the 22 novel derivatives was assessed on Haspin kinase. Two of them possessed an IC₅₀ of 1 and 2 nM with selectivity towards a panel of 10 other kinases including the parent kinases DYRK1A and CLK1. The most selective compound exerted additionally a very interesting cell effect on the osteosarcoma U-2 OS cell line.

ARTICLE HISTORY

Received 8 March 2021
Revised 11 May 2022
Accepted 22 May 2022

KEYWORDS

Indoloquinoline; Haspin kinase; docking; cell viability

Introduction

Marine products currently represent an underutilised source of leads for the pharmaceutical industry¹. Besides their original and complex structures, they often offer new action modes and structural originality. Nevertheless, their low abundance and the presence of few analogues makes it difficult to obtain large libraries, perform full biological characterisation and achieve structure–activity relationship (SAR) exploration. Despite these difficulties, these products remain attractive due to their high valorisation potential, and their complex structures have prompted medicinal chemists to use disruptive strategies to intuitively isolate the pharmacophore elements that trigger biological activity.

For these reasons, some marine products and their synthetic analogues have emerged in drug discovery strategies and several of them have been reported for protein kinase inhibition². Among them the most successful example is the polycyclic staurosporine **I**^{3,4}. This lead compound has led from extraction, hemisynthesis and organic synthesis efforts to Lestaurtinib **II**^{5,6} and simplified Enzastaurin **III**⁷, two potent drugs targeting VEGF receptors and kinases, which have entered clinical trials against leukaemia and cancer (Figure 1). In this field, the chemical simplification of indolocarbazole scaffolds and caulersin **IV** have generated strong kinase inhibitors and cytotoxic agents^{8–14}.

Among these bis-indole series, lamellarins, a group of pyrrole alkaloids, have emerged (Figure 2)^{15,16}. These compounds are a class of marine-derived natural products isolated from molluscs, ascidians and marine sponges. Nearly, 70 natural derivatives have been reported in this family which mainly contains a fused pentacyclic pyrroloisoquinoline lactone ring system¹⁷. Lamellarins have

focused the attention of medicinal chemists due to their diverse biological effects. Some have demonstrated cytotoxic activities and multidrug resistance (MDR) reversal in a number of cancer cell lines, as well as being confirmed inhibitors of topoisomerase I. Moreover, Lamellarins **D** (structure **V**, Figure 2), **N** and **L** have proved their ability to inhibit kinases such as GSK3 β , DYRK1A and CDK5 in the nanomolar range¹⁸. Our first approach in this chemical series was based on the simplification of the synthetic model in order to discriminate the two activities, that is, diminish the topoisomerase I inhibition while retaining the kinase inhibition by fine-tuning the chemical structure.

This objective was reached by replacing the pyrrole moiety with an indole skeleton and designing new chromeno[3,4-b]indoles **VI** which revealed DYRK1A inhibition. In this structure, the rings of Lamellarin-D noted A, B and C were unchanged (Figure 2). Despite structural modulations, the kinase inhibition remained mainly in the sub-micromolar range except for derivatives **1a** and **1b**, which exhibited a high selective inhibition of DYRK1A but revealed instability in basic media due to the lactone. We therefore decided to develop a more robust indoloquinoline^{19–23} series **VII** with the objective of creating a novel and druggable family of kinase inhibitors, as we envisioned that the presence of lactam combined with the NH of pyrrole would reinforce the hydrogen bond donor acceptor binding mode to the ATP active site.

Herein, we present access to the indolo[2,3-c]quinolone-6-one library and the evaluation of the family on a representative panel of kinases involved in CNS, inflammatory diseases and oncology. SAR are depicted and we demonstrate that in

CONTACT Cleopatra Neagoie ✉ cleopatra.neagoie@crmh-cas.org.hk Centre for Regenerative Medicine and Health, Hong Kong Institute of Science and Innovation, Chinese Academy of Science, Hong Kong SAR, China

Supplemental data for this article can be accessed online at <https://doi.org/10.1080/14756366.2022.2082419>.

© 2022 The Author(s). Published by Informa UK Limited, trading as Taylor & Francis Group.

This is an Open Access article distributed under the terms of the Creative Commons Attribution License (<http://creativecommons.org/licenses/by/4.0/>), which permits unrestricted use, distribution, and reproduction in any medium, provided the original work is properly cited.

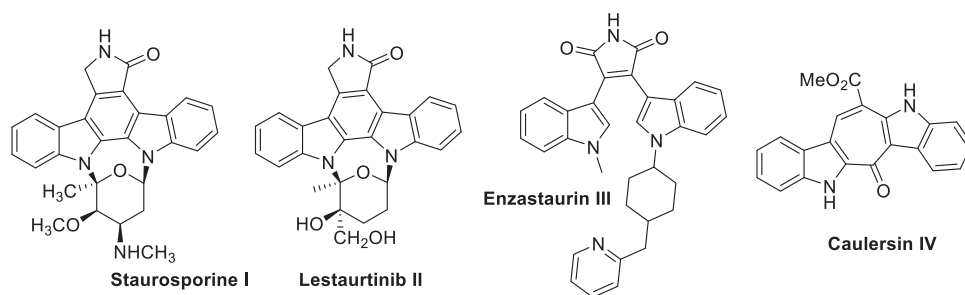


Figure 1. Structures of Staurosporine and its simplified derivatives, which have entered clinical trials as kinase inhibitors, and Caulersin.

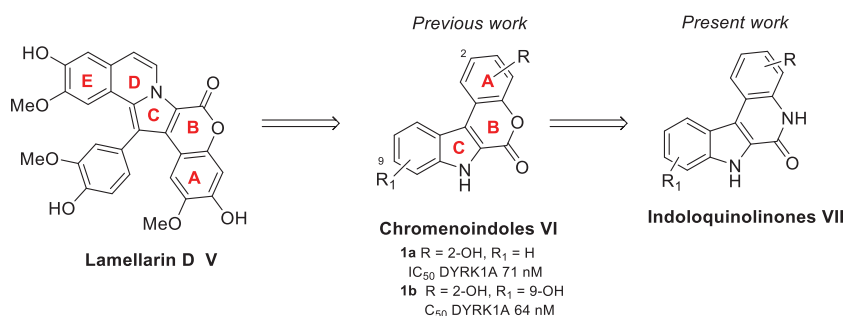
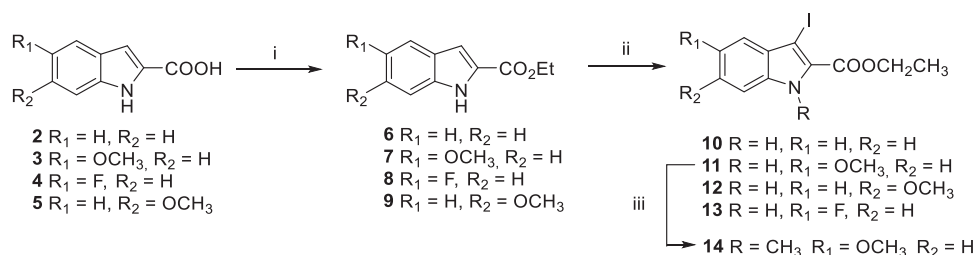
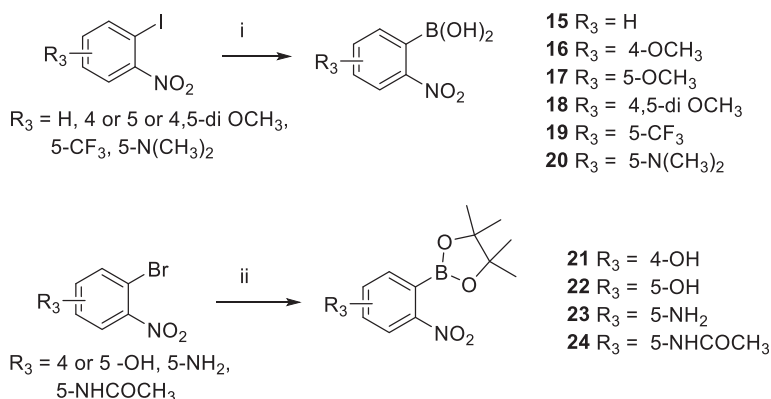


Figure 2. Lamellarin D, chromenoindoles, and envisioned indoloquinolinone chemical series.



Scheme 1. Reagents and conditions: (i) EtOH, conc. H₂SO₄ 10 mol%, reflux, 12 h, **6–9** quant; (ii) I₂ (1.5 equiv.), KOH (4.0 equiv.), DMF, r.t., 4 h; (iii) NaH (1.5 equiv.), CH₃I (1.2 equiv.), DMF, 0–20 °C.

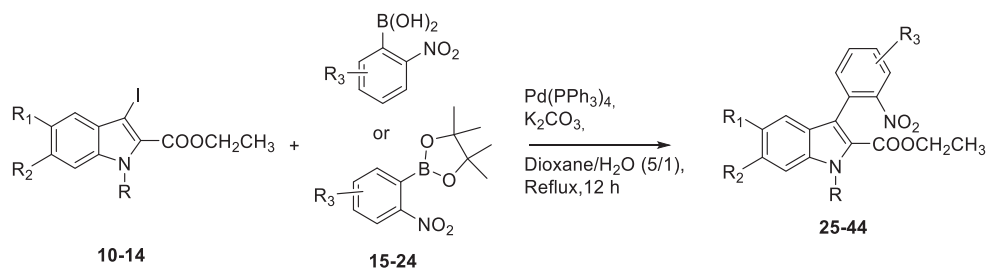


Scheme 2. Reagents and conditions: (i) PhMgCl 2 M in THF (1.2 equiv.), B(OCH₃)₃ (1.2 equiv.), 30 min. at -78 °C, then aq. HCl 2 M at -10 °C, 10 min; (ii) PdCl₂(dppf) (0.03 equiv.), KOAc (2.0 equiv.), Bis-(pinacolato)diboron (1.5 equiv.), 1,4-dioxane/H₂O 10/1, 80 °C, 14 h.

addition to retaining DYRK1A inhibition to a large extent, other molecules acting on CLK1 have also been designed. We additionally found that several compounds inhibit the Haspin kinase with an unprecedented selectivity. Molecular docking experiments were conducted to explain these results. Finally, screening on a cancer cell line was carried out and results showed that the compounds induced cellular effects and affect osteosarcoma cell lines in particular.

Chemistry

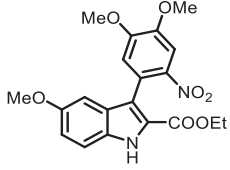
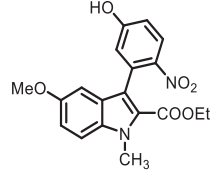
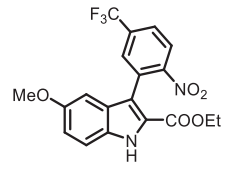
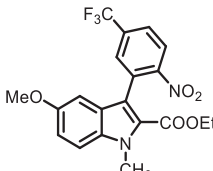
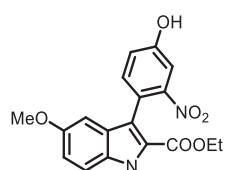
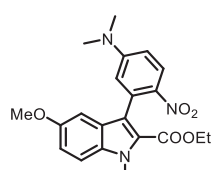
In order to introduce ring A on the indole, a Suzuki-Miyaura reaction appeared to be the most appropriate. The 3-iodoindole-2-carboxylic ethyl esters **10–13** were therefore prepared after 2 efficient steps. The first one consisted in the quantitative esterification of **2–4** using 10 mol% of sulphuric acid catalyst in ethanol, followed by iodination in presence of KOH to afford the attempted ethyl 3-iodo-1*H*-indolo-2-carboxylates²⁴. Noteworthy, the *N*-methylation of indole **11** with a

Table 1. Suzuki-Miyaura reaction using **10–14** and boronylated derivatives **15–24**.

Entry	Starting materials	Product ^a (Formula/number)	Entry	Starting materials	Product ^a (Formula/number)
1	10 + 15		11	11 + 22	
2	10 + 17		12	11 + 23	
3	10 + 21		13	11 + 24	
4	10 + 22		14	12 + 15	
5	11 + 15		15	12 + 17	
6	11 + 16		16	13 + 17	
7	11 + 17		17	13 + 22	

(continued)

Table 1. Continued.

Entry	Starting materials	Product ^a (Formula/number)	Entry	Starting materials	Product ^a (Formula/number)
8	11 + 18	 32	18	14 + 22	 42
9	11 + 19	 33	19	14 + 19	 43
10	11 + 21	 34	20	14 + 20	 44

^aYields are indicated in the experimental section.

slight excess of iodomethane in presence of sodium hydride gave **14** in a near quantitative yield (Scheme 1).

Next, we focussed on preparing the second partner for the cross coupling reaction, that is, the unavailable boronated nitrobenzene derivatives (Scheme 2). When the starting 2-halogeno nitrobenzenes do not contain any acidic proton, the use of Grignard reagent is recommended in the literature²⁵. The reaction was first carried out with phenyl magnesium chloride (1.2 equiv.) in presence of methylorthoborate as electrophile whereas a final acidic hydrolysis led to the desired 2-nitroaryl boronic acids **15–20** in fair good yields. When 2-halogeno nitrobenzenes bear an acidic proton, the Miyaura borylation reaction can be used with conditions involving PdCl₂(dppf) as catalyst and potassium acetate as a base in dioxane. This method furnished pinacol boronic esters **21–24** with modest yields after 14 h of reaction at 80 °C. Due to their sensitivity during the purification step, the boron derivatives were used in the cross coupling reaction as crude materials.

Assembly of the two building blocks was next performed using the Suzuki-Miyaura reaction in presence of PdCl₂(dppf) and potassium carbonate as base in a refluxing mixture of water and dioxane. These conditions proved fully suitable to achieve all the envisioned cross couplings and the desired derivatives were isolated with yields ranging between 40 and 60% after 12 h of reaction (Table 1). Finally, we thought that the large library of final compounds **45–64** could be obtained by a “one pot” strategy (Table 2). To this end, the nitro derivatives **25–44** were also treated with iron powder in refluxing acetic acid and the *in situ* formed amine concomitantly formed the lactam ring by annelation with the nearby ethyl ester. An original library of substituted 5,7-dihydro-6H-indolo[2,3-c]quinolin-6-ones **45–65** was obtained with very high yields.

Kinase assays, SAR

We previously showed that analogues of Lamellarin D, chromeno[3,4-*b*]indoles, had the ability to inhibit the DYRK1A kinase¹⁵

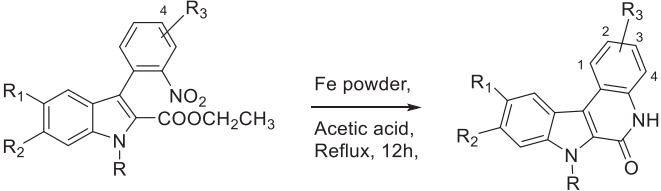
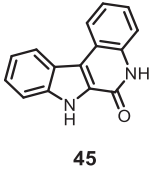
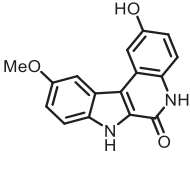
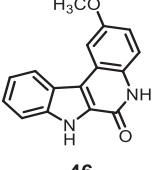
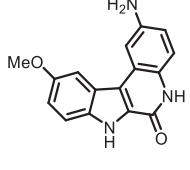
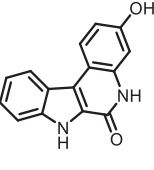
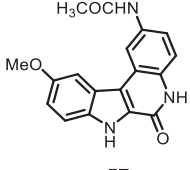
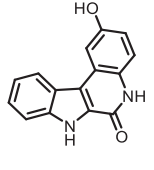
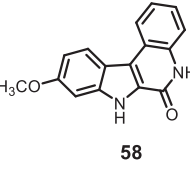
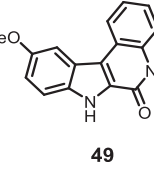
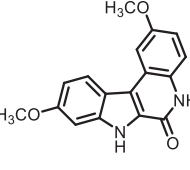
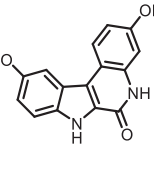
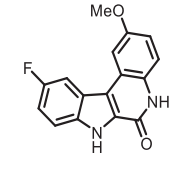
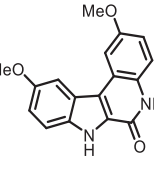
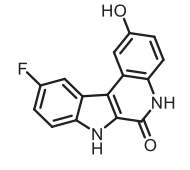
and it has been shown by different groups that DYRK inhibitors often cross-react with CLKs and with the mitotic kinase Haspin^{26,27}. We therefore tested the inhibitory activity of the 22 synthesised derivatives on the *Hs*Haspin, *Mm*CLK1 and *Rn*DYRK1A recombinant kinases (Table 3).

The selectivity of each derivative was also determined on a representative kinase panel including *Hs*Cdk2/Cyc A, *Hs*Cdk5/p25, *Hs*Cdk9/Cyc E, *Hs*GSK3 β and *Hs*PIM1. Interestingly, more than half of the analogues displayed very high activity towards Haspin with a percentage of residual activity at 1 μ M close to zero (ranging from 6% for compound **46** to 0% for compounds **61**, **54**, **55**, and **62**). Apart from 5 compounds (**45**, **58**, **47**, **53**, **63**, and **64**), 17 novel indoloquinolinones showed an interesting selectivity towards Haspin, CLK1 and DYRK1A kinases with moderate activity on CDKs, GSK-3 β and PIM1.

IC₅₀ for Haspin, CLK1 and DYRK1A were next calculated for 14 compounds showing residual kinase activity \leq 25% on Haspin kinase at a concentration of 1 μ M (Table 4). It clearly appeared that the lactam moiety favoured DYRK1A inhibition. While the hydroxylated derivatives **1a** and **1b** displayed good activity on DYRK1A, they are nevertheless the only molecules in their family to present this action whereas the 14 lactams reported in this study exhibited an inhibition below 300 nM. It is possible that due to the electro-donating lactam nitrogen atom (vs. the O of the lactone), the electron density on the carbonyl group is sufficiently modified to strengthen a favourable hydrogen bond in the active site (see molecular modelling studies). Moreover, the compounds **48**, **49**, and **51** (entries 2, 3, 5) appear to be the best DYRK1A inhibitors of the series with more potent IC₅₀ than the lactones **1a** and **1b** (entry 1).

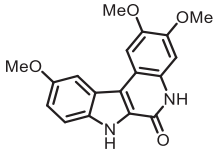
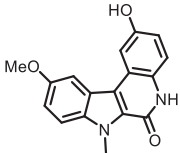
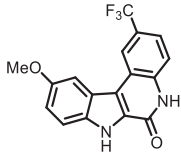
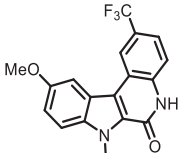
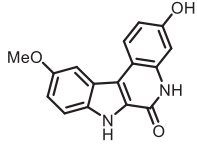
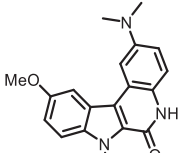
The concomitant action of DYRK1A inhibitors with CLK1 was confirmed since most of the Haspin inhibitors were also active on DYRK1A and CLK1. The mode of interaction of **49**, which is highly active on Haspin and exhibits strong activity on the other two kinases, was studied by molecular docking experiments (see Molecular docking studies section). Considering the two enzymes

Table 2. "One pot" reduction of nitro group and lactam formation of derivatives **25–44** leading to final compounds **45–64**.

					
Entry	Starting materials	Product ^a (Formula/number)	Entry	Starting materials	Product ^a (Formula/number)
1	25	 45	11	35	 55
2	26	 46	12	36	 56
3	27	 47	13	37	 57
4	28	 48	14	38	 58
5	29	 49	15	39	 59
6	30	 50	16	40	 60
7	31	 51	17	41	 61

(continued)

Table 2. Continued.

Entry	Starting materials	Product ^a (Formula/number)	Entry	Starting materials	Product ^a (Formula/number)
8	32		18	42	
9	33		19	43	
10	34		20	44	

^aYields are indicated in the experimental section.Table 3. Residual activity on a representative panel of 8 protein kinases at 1 μ M.

Entry	Compound	% Residual activity at 1 μ M ^a							
		Haspin	CLK1	DYRK1A	CDK2	CDK5	CDK9	GSK3 β	PIM1
1	45	44	67	61	100	100	63	100	86
2	46	6	13	18	80	78	62	86	32
3	47	28	22	33	61	59	20	47	37
4	48	1	4	12	84	87	49	100	63
5	49	2	5	7	73	77	40	39	41
6	50	3	10	5	77	81	51	44	19
7	51	1	5	14	62	70	33	29	36
8	52	2	1	5	58	63	37	22	29
9	53	33	11	36	76	56	56	63	31
10	54	0	11	2	35	59	18	48	9
11	55	0	14	2	38	53	17	20	22
12	56	2	3	7	72	79	37	39	65
13	57	3	2	10	100	100	72	58	37
14	58	59	49	55	62	55	55	51	48
15	59	13	12	21	74	51	41	41	34
18	60	9	31	44	97	100	100	100	100
19	61	0	2	9	57	91	41	71	38
20	62	0	0	2	31	22	6	31	75
21	63	51	19	29	67	68	45	44	42
22	64	39	11	19	100	100	59	81	82

^aResidual kinase activity was determined at 1 μ M concentration for each compound. The data mean ($n=2$) expressed as percentage of maximum activity of the DMSO control.

we can say that compounds **48** and **49** inhibit DYRK1A and CLK1 almost equally in the nanomolar range.

As regards to Haspin inhibition, the chemical series of type **VII** is of great interest. Eight compounds showed an IC_{50} below 10 nM. Compound **45** (Table 3, entry 1), without any substituent on the aromatic parts, presented no kinase activity. To maximise the inhibition, at least one methoxy OCH_3 or hydroxy OH group is required in positions C-2 or C-3 (compounds **46**, **48**, **50**, **51**, **54**,

55, **61**), the amino derivatives or amides being less effective (Table 4, entries 9 and 10).

Regarding the indole ring substituents, the absence of a substituent or the presence of an OCH_3 or a fluorine in C-10 position did not significantly affect the Haspin inhibition (products **46**, **51** and **61**, entries 1, 5, 13) when a functional group was also present on the C-2 or C-3 positions of the phenyl ring. Finally, the presence of ether in position C-9 (entry 11 vs. 5) or the methylation of indole (entry 14 vs. 5) made the compounds less effective.

The inhibitory activity of compound **49** on Haspin was about 12 times stronger than that of the other two enzymes. At 20 nM this molecule inhibited the 3 enzymes quantitatively. Compound **55** showed an even higher selectivity since the selectivity for CLK1 was identical, but against DYRK1A it rose to a factor of 65. At this stage, we can almost say that at a dose of 20 nM, this molecule shows a dual inhibition of Haspin and CLK1.

We further evaluated the selectivity profile of compound **55** on a larger panel of kinases (SelectScreen Whole Panel, Life Technologies). The inhibition profile of **55**, evaluated at 1 μ M, is depicted on a dendrogram on Figure 3 where kinases inhibited by a minimum of 80% are shown. A full list of the kinases tested is shown on Table S1 in supplementary information.

The inhibitory activities of compound **55** on Haspin, CLKs and DYRKs are well found in this new screening study. Product **55** is not specific but appears to be relatively selective since the compound **55** (AS-N14) presents a reasonable selectivity profile against a panel of 486 tested kinases since it inhibits 73 of the 486 kinases by >80%, and 159 of the 486 kinases by >50% at a dose of 1 μ M.

Molecular docking studies

Molecular docking studies were carried out using Glide^{28–30} from the Schrödinger Suite³¹, in order to compare putative binding

Table 4. Measured IC₅₀ values (nM) on Haspin, CLK1 and DYRK1A.

Entry	Compound	Kinase inhibition (IC ₅₀) ^a (IC ₅₀ in nM)			Selectivity index	
		Haspin	CLK1	DYRK1A	CLK1/Haspin	DYRK/Haspin
Ref	1a	ND	ND	74	ND	ND
Ref	1b	ND	ND	67	ND	ND
1	46	7	51	68	7	10
2	48	6	17	19	3	3
3	49	1	13	15	13	15
4	50	7	88	196	13	28
5	51	4	10	41	3	10
6	52	16	78	242	5	15
7	54	4	82	97	21	24
8	55	2	33	130	17	65
9	56	14	213	226	15	16
10	57	34	259	280	8	8
11	59	30	94	73	3	2
12	60	19	122	143	6	8
13	61	5	78	104	16	21
14	62	18	124	131	7	7

^aIC₅₀ values were determined on Haspin, CLK1 and DYRK1A when the residual kinase activity was ≤25% on Haspin at a compound concentration of 1 μM in Table 3. They were calculated from a dose-response curve for which each point was measured in duplicate, and reported in nM. Selectivity indexes (SI) were calculated as follows: IC₅₀ DYRK1A or CLK1/IC₅₀ Haspin.

Table 5. Effects on cell viability, EC₅₀ on RPE1 and U-2 OS cell lines^a.

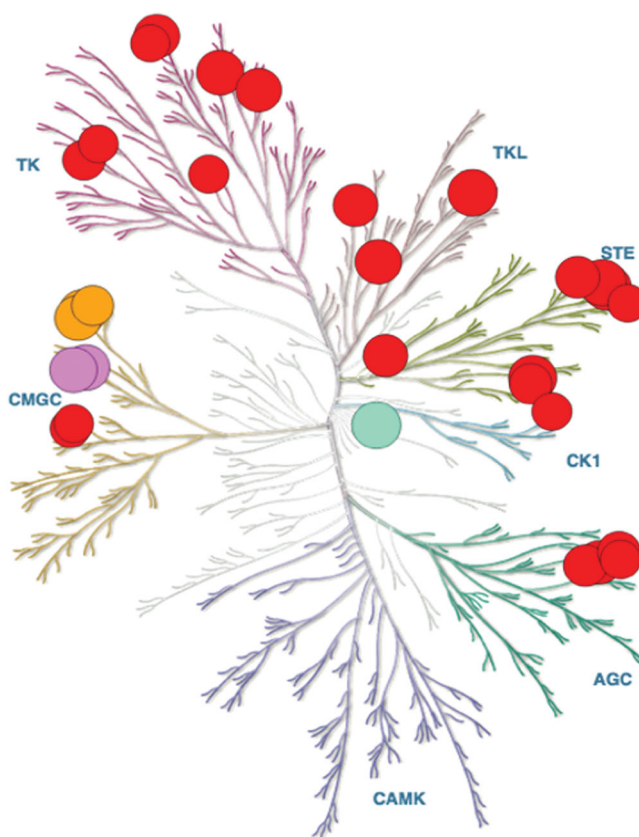
Entry	Compound	RPE1 EC ₅₀ in μM	U-2 OS EC ₅₀ in μM
1	46	>25	>25
2	48	7.3	7
3	49	>25	>25
4	50	20.8	4.3
5	51	>25	12.6
6	54	>25	>25
7	55	10.7	3.4
8	56	>25	>25
9	61	19.1	8.7

^aCells were incubated with increasing doses of each compound (up to 50 μM) for 48 h. Cell viability was determined by MTS assay in triplicate and EC₅₀ (μM) were calculated from the dose-response curves.

modes and explore interactions within the active sites of CLK1, DYRK1A and Haspin kinases. Active sites of the three crystal structures were superimposed and are shown in Figure 4. The residues engaging hydrogen bond interactions with docked ligands are highlighted in stick form.

One of the most active compounds, **49** was docked in each active site of the three kinases. The docking poses exhibited the same putative binding mode, highlighting a hydrogen bond between the acceptor atom O of the lactam ring of **49** and the backbone of the hinge Leu244 (CLK1), Leu241 (DYRK1A) and Gly608 (Haspin). In addition, **49** formed another interaction with the hinge region of Haspin through a hydrogen bond between NH of the lactam ring and the backbone of Gly609 (Figure 4). In some docking poses, the molecule was flipped by 180° exposing the methoxy group of **49** towards the solvent area.

Derivatives **51** and **62** were next docked in order to investigate the studied binding mode in greater depth since **62** has an



"Illustration reproduced courtesy of Cell Signalling Technology, Inc. (www.cellsignal.com)"

Figure 3. Selectivity profile of compound **55** evaluated on 486 kinases at 1 μM in duplicate (SelectScreen Whole Panel, Life Technologies) and represented on a dendrogram (courtesy of Cell Signalling Technology). Kinases whose activities are inhibited by 80% and above are shown as dots, Haspin is visualised as a green dot, CLKs as purple dots and DYRKs as orange dots.

N-methyl group on the pyrrole moiety. The best docking poses of the two compounds **51** and **62** were similar to **49** (Figure 5). No steric clash between the protein and the second methoxy group of the ligand was observed. Interestingly, **62** compared to **51** showed a weak H-pi interaction between the methyl group of the indole moiety and the gatekeeper, Phe605, of the kinase. The presence of the methyl group in **62** did not impact the binding mode of the compound, which explains the acceptable IC₅₀ of **62**.

From the docking experiments, we predicted that the binding mode in each protein kinase, Haspin, CLK1 and DYRK1A, would be very similar. Nevertheless, as in most docking experiments, the docking score is not sufficient to predict the small variation in activity of the compounds and further intensive computational approaches such as free energy of binding (FEB) would be needed.

Cell assays

We next analysed the effects of selected compounds (Haspin IC₅₀ <15 nM) on the cell viability of several cell lines from osteosarcoma (U-2 OS), colorectal cancer (HCT116), breast cancer (MDA-MB231) and neuroblastoma (SH-SY5Y) as well as retinal fibroblast RPE-1 immortalised with hTERT (Figure 6). In a primary screen, all compounds were tested in triplicate at 25 μM and viability was expressed as percentage of a DMSO control. U-2 OS and HCT116 cell lines appeared to be the most sensitive to our compounds and were even slightly more affected than the non-cancerous

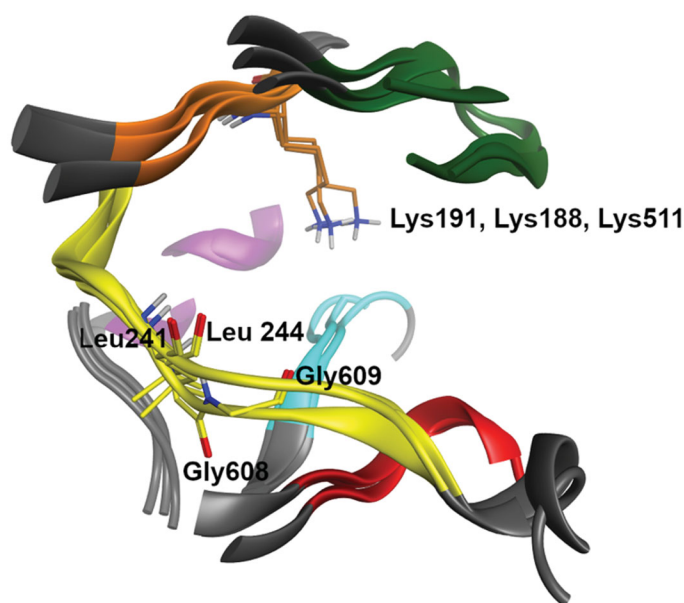


Figure 4. Superimposition of the ATP site of the three protein kinases, CLK1, DYRK1A and Haspin (residues and ribbons are coloured regarding their localisation in the kinase structure: hinge region (yellow), DFG motif (cyan), G loop (green), Catalytic K (orange), α C-helix (purple) and HRD region (red)), drawn with MOE software.²⁴ Non-polar hydrogen atoms are hidden for clarity. Catalytic lysine and residues in the hinge region forming hydrogen bonds with the ligand are highlighted. CLK1: Leu244 and Lys191, DYRK1A: Leu241 and Lys188, and Haspin: Gly608, Gly609 and Lys 511.

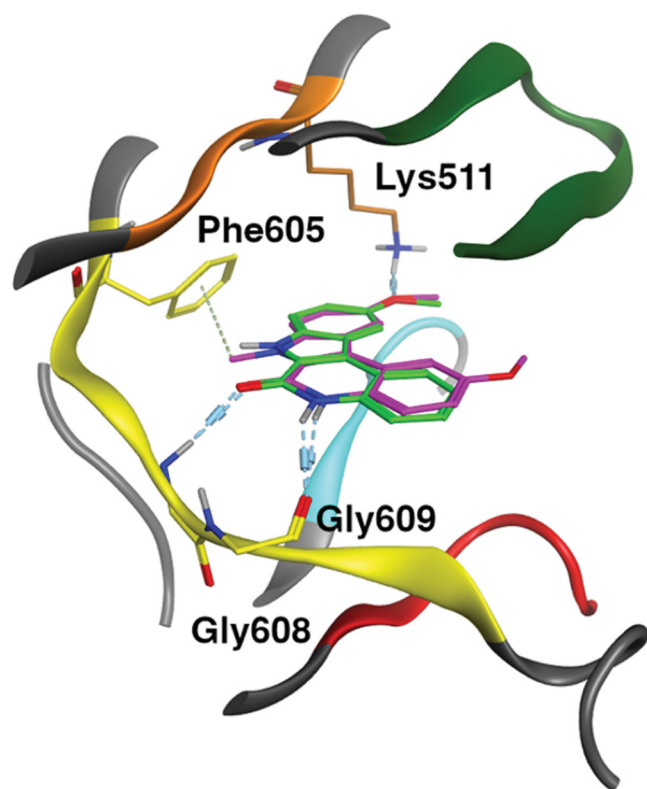


Figure 5. Binding mode representation of **49** (green) and **62** (purple) in ATP site of Haspin. Hydrogen bond interactions are represented in dashed lines.

RPE-1 cell line, whereas the SH-SY5Y and MDA-MB231 cell lines emerged as the most resistant ones. Compounds **46**, **49**, **51**, **54**, and **56** had little to no effect on all the tested cell lines. This can

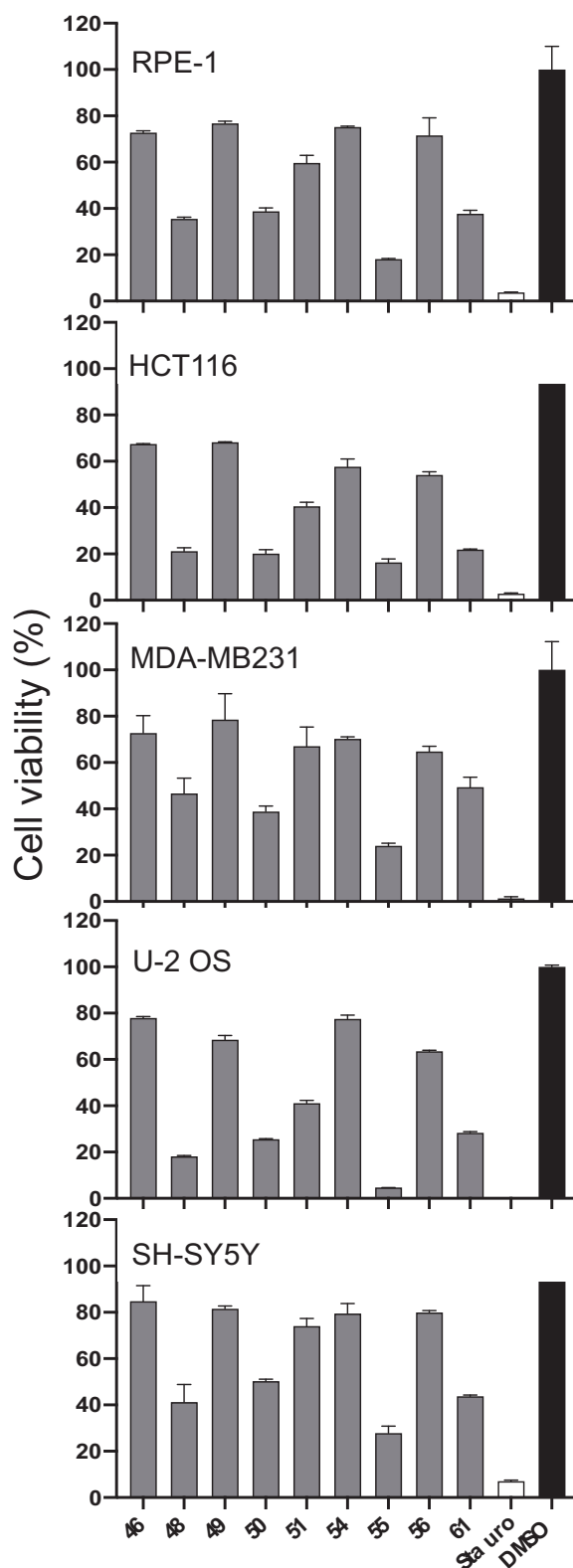


Figure 6. Effects of compounds on cell viability. Cell viability was assessed on the following human cell lines: U-2 OS (osteosarcoma), HCT116 (colorectal cancer), MDA-MB231 (breast cancer), SH-SY5Y (neuroblastoma) and RPE-1 (retinal fibroblast immortalised with hTERT). Cells were incubated with 25 μ M of selected compounds or 10 μ M of staurosporine or 0.1% of DMSO for 48 h. Cell viability was evaluated in triplicate via MST assay and results expressed as percentage of DMSO control (mean set at 100%). Results on graphs are mean \pm SD.

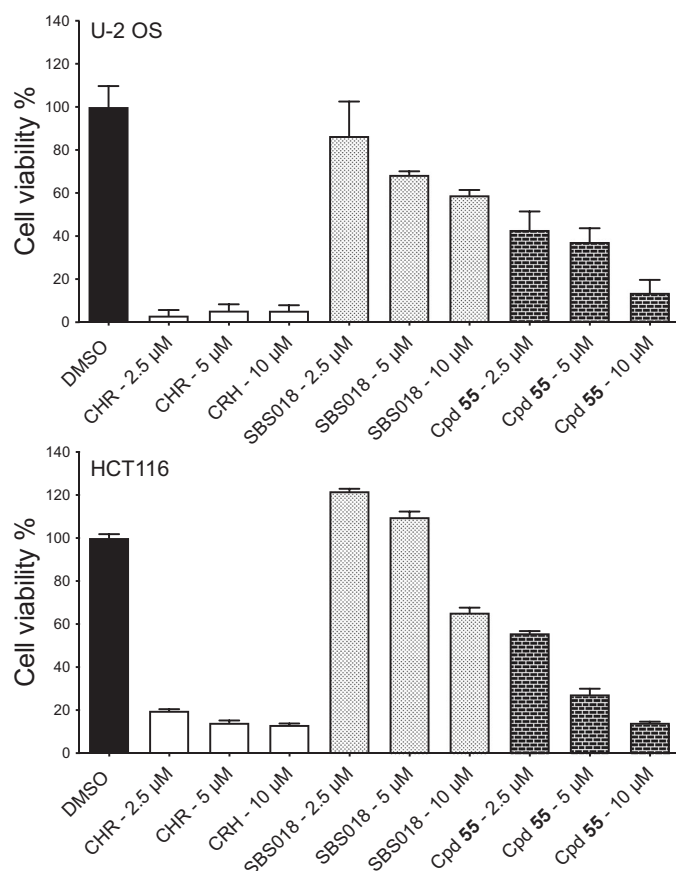


Figure 7. Effects of compounds on U-2 OS and HCT116 spheroid viability. Cell viability in spheroids from U-2 OS and HCT116 cells was measured after 7 days of treatment with DMSO (0.5%), CHR6494 (CHR), SBS018 or Cpd55 at a single dose of 2.5, 5, and 10 μ M, on day 0. Cell viability is expressed in percentage of the DMSO control. $n = 3$, results are mean \pm s.e.m.

be explained by the low solubility of the compounds, or their low affinity for lipidic plasma membrane or a high metabolism rate in aqueous solution/cellular environment. On the other hand, several compounds such as **48**, **61**, **55**, and **50** showed a reduction of equal or more than 75% of cell viability compared to the DMSO control.

Hence, dose-response experiments were carried out on both U-2 OS and RPE-1 cell lines and EC_{50} were calculated (Table 5). The results confirmed the lack of efficacy of compounds **46**, **49**, **54**, and **56** which showed $EC_{50} > 25 \mu$ M on both cell lines regardless of their activity on Haspin kinase (IC_{50} of 7, 1, 4 and 14 nM respectively). Derivative **51**, despite no effect observed on RPE-1 cells ($EC_{50} > 25 \mu$ M), showed a moderate activity on cell viability of the U-2 OS line with an EC_{50} of 12.6 μ M. The compounds were generally more efficient at inhibiting the viability of U-2 OS cancerous cells than that of normal RPE-1. Amongst the selected compounds, **55** and **50** displayed the strongest effect on the viability of U-2 OS cells (EC_{50} of 3.4 and 4.3 μ M, respectively). They were between 2 and 5 times more active on U-2 OS compared to RPE-1 cell viability.

Taken together, these results showed that some of our compounds such as **55** and **50** displayed interesting effects on cell viability of several cancerous cell lines.

We further examined the effect of our most efficient compound (**55**) on cancerous cells growing in 3D spheroids. U-2 OS and HCT116 cells spheroids were prepared and treated with different concentrations of either compound **55**, CHR-6494 or SBS018 (compound **21** in ref Elie et al)²⁶ or with 0.5% DMSO for 7 days,

after which, spheroids viability was evaluated (Figure 7). We observed a marked dose-dependent effect of compound **55** on both U-2 OS and HCT116 spheroid cell viability after 7 days of treatment. This effect was milder than the one observed with CHR-6494 and stronger than the one induced by SBS018 at similar concentrations.

We further characterised the functional effects of our most efficient compound **55** on endogenous Haspin in U-2 OS cells by immunofluorescence, quantifying the Haspin specific H3T3ph signal in early mitotic cells. The H3T3ph signal was measured on cells treated with 0.5 μ M of compound **55** or CHR-6494 or SBS018 or with 0.1% of DMSO for 16 h (Figure 8). Our results showed that compound **55** could inhibit intracellular Haspin with a very similar efficiency to that of CHR-6494 or SBS018. These results further validate the functionality of our compound in cells, on the endogenous Haspin kinase activity.

We then characterised the effect of compound **55** on the cell cycle on U-2 OS cells. Cells were treated for 24 h with 1 μ M of compound **55**, CHR-6494, SBS018 or DMSO at 0.2% and their cell cycle profile was analysed by flow cytometry (Figure 9). Analysis of flow cytometry profiles showed, as expected, a strong increase in the percentage of cells in G2/M phase of the cell cycle with compound **55** as well as with the two references CHR-6494 and SBS018 compared to the DMSO control (20, 17, and 14%, respectively vs. 6% for the DMSO control). Concomitantly, compound **55** further induced a reduction of cells in the G1 phase compared to the control (36 vs. 50%, respectively), an expected result of the strong observed G2/M delay. These results are consistent with an impaired Haspin function inducing prolonged mitoses as previously described (Huertas et al. 2012; Peiling Wang et al. 2021/ PMID:34551143).

Conclusion

We have synthesised a series of new Lamellarin analogues using the indolo[2,3-*c*]quinolone-6-one core. The analogues were obtained after a sequence involving (i) a palladium catalysed cross coupling reaction between 2-indolic esters and 2-nitrophenyl boronic acids as building blocks, and (ii) a cyclic lactam formation involving a reduction and an annelation. Twenty-two novel derivatives were synthesised and evaluated for their inhibitory activity on Haspin kinase and on a panel of 7 other protein kinases for selectivity assessment. Among this series, 8 compounds inhibited Haspin kinase with IC_{50} below 10 nM. Docking studies showed a double hydrogen bond between the lactam and the hinge region of the kinase. The most active compounds **49** and **55** possess IC_{50} of 1 and 2 nM respectively with selectivity towards the parent kinases DYRK1A and CLK1 between a 13 and 65-fold factor. Furthermore, the most selective compound **55** exerted an interesting cellular effect on the osteosarcoma U-2 OS cell line as well as on U-2 OS and colorectal carcinoma HCT116 spheroid viability. Additionally, we further validated the functionality of compound **55** on endogenous Haspin activity in cells. This interesting Haspin inhibitor will be used in further studies to develop efficient and selective Haspin inhibitors.

Experimental section

Chemistry

All reagents and solvents were purchased from commercial sources and used without further purification. 1H NMR and ^{13}C NMR spectra were recorded on 400 MHz and/or 500 MHz Bruker FT-NMR spectrometers. All chemical shifts are given as δ values

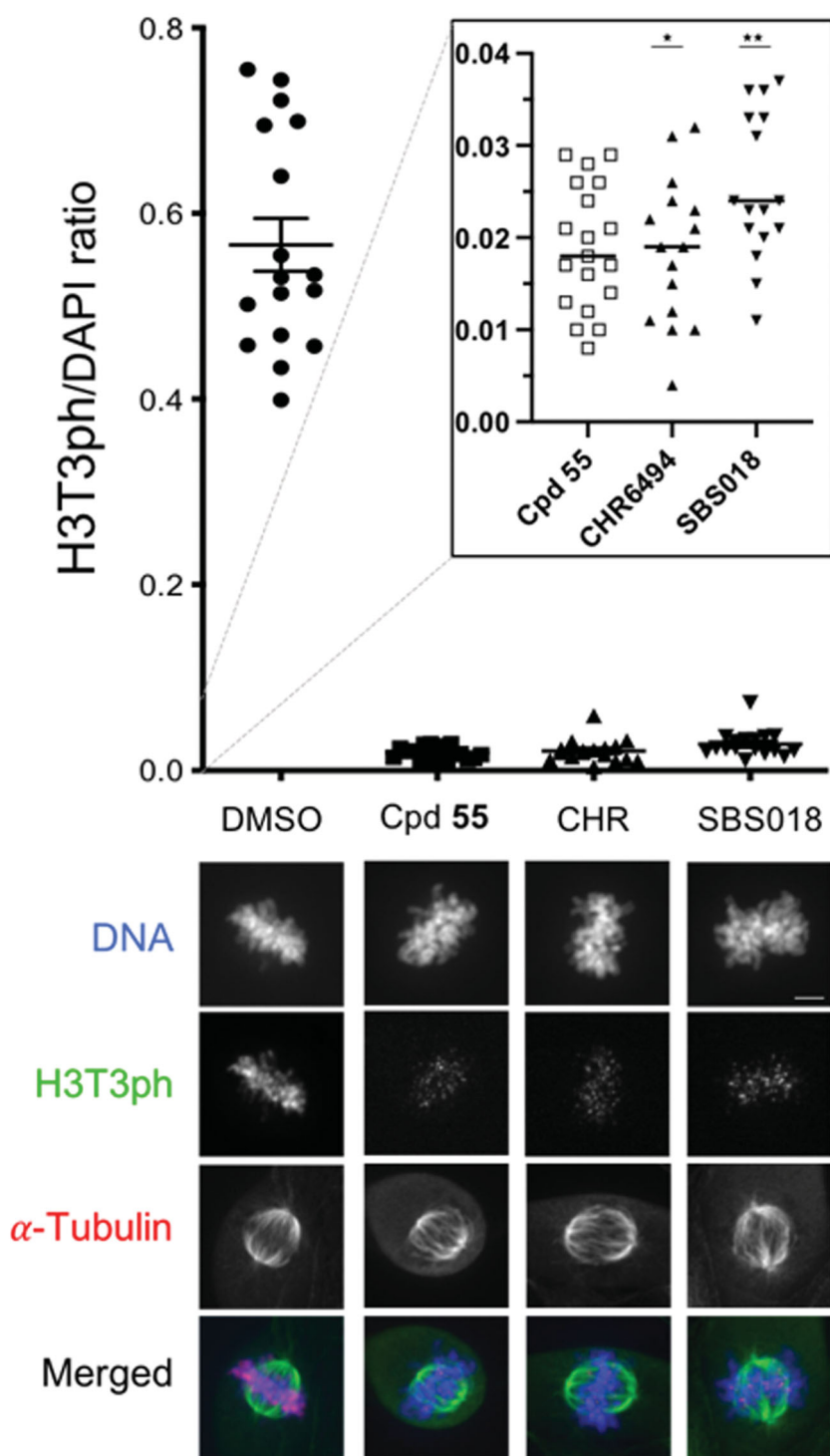


Figure 8. Cellular endogenous Haspin inhibition. U-2 OS cells were treated for 16 h with 0.5 μ M of each compound or 0.1% of DMSO (CHR: CHR-6494). Haspin activity was monitored by immunofluorescence staining of phosphorylated Histone H3 on threonine 3 (H3T3ph, green); α -Tubulin was visualised in red and DNA was stained by DAPI (blue). Haspin activity was quantified in prometaphase/metaphase cells measuring the H3T3ph and DAPI signals and representing the H3T3ph/DAPI ratio on a scatter plot (upper panel). The inserted dot plot allows the comparison of the 3 tested compounds on a more precise scale; $n \geq 15$, $*p \leq 0.05$; $**p \leq 0.01$ (two-tailed unpaired t-test). Representative images are presented on the lower panel, Bar 5 μ m.

(ppm) with reference to tetramethylsilane (TMS = 0) as an internal standard. The peak patterns are indicated as follows: s, singlet; d, doublet; t, triplet; m, multiplet; q, quartette. The coupling constants, J , are reported in Hertz (Hz). UV detection at 210 nm. High resolution mass (MS) analysis was conducted using an LC/MSD TOF spectrometer system with electrospray ionisation (ESI). Reactions were monitored via thin-layer chromatography (TLC) carried out on commercial silica gel plates (GF254) under UV light.

Column chromatography was performed on silica gel 60 (200–300 mesh).

General procedure A: preparation of 3-iodoindoles (11–13)

Indole-2-carboxylic acid derivatives (3.1 mmol) were dissolved in Ethanol (50 ml) and conc. sulphuric acid (5 ml) was added. The solution was refluxed for about 12 h (monitoring with TLC) after

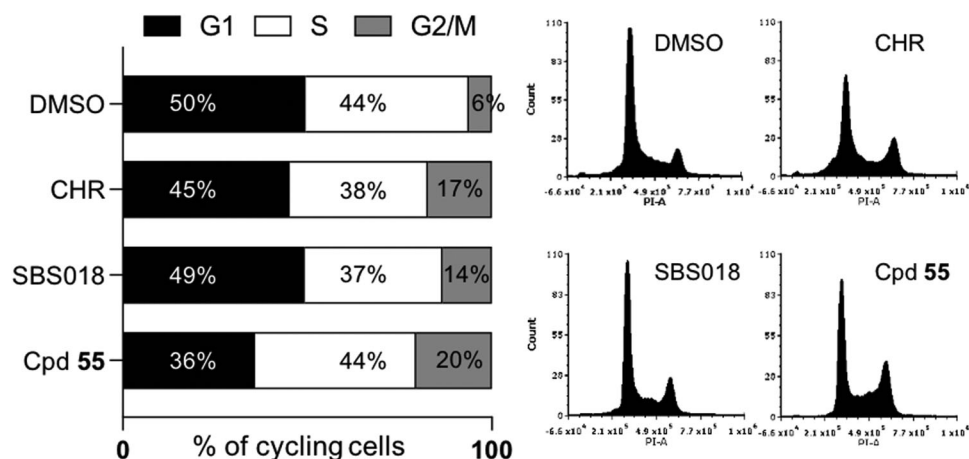


Figure 9. Effect of compounds on the cell cycle. U-2 OS cells were treated for 24 h with 1 μ M of each compound or 0.2% DMSO (CHR: CHR-6494). DNA content was measured by flow cytometry and the percentages of cells in each phase of the cell cycle is represented on a proportional bar graph. Representative profiles for each treatment are shown on the right panels.

completion of the reaction. The solution was poured into cold water (150 ml), and the white solid precipitate formed was collected by filtration. The solid material was washed with water and dried to produce quantitatively derivatives **6–9**. Crude materials were next dissolved in a mixture containing crushed KOH (4.0 equiv.) pellets in DMF (15 ml) at room temperature. Next Iodine (1.5 equiv.) dissolved in DMF (3 ml) was added dropwise and the mixture stirred for 4 h at room temperature (monitored with TLC). After completion (TLC monitoring), the reaction mixture was poured onto a saturated aqueous solution of NaHSO₃ (15 ml), NH₄OH (30%, 2 ml) and water (15 ml). The solid was filtered, dried under reduced pressure, and used directly without further purification. All spectral data for **10**, **11**, **13** are in agreement with previous reports [20, 21]. Compounds **11–13** were engaged immediately in the next step.

Ethyl 3-iodo-6-methoxy-1H-indole-2-carboxylate (**12**)

Compound **12** was isolated as a white solid (81%) starting from **8** following the general procedure A. ¹H NMR (CDCl₃, 400 MHz) 1.23 (t, *J* = 7.2 Hz, 3H), 4.25 (q, *J* = 7.2 Hz, 2H), 3.99 (s, 3H), 7.05 (s, 1H), 7.20 (d, *J* = 7.4 Hz, 1H), 8.10 (d, *J* = 7.4 Hz, 1H), 11.55 (s, 1H). ¹³C NMR (CDCl₃, 125 MHz) 14.4, 55.6, 61.3, 66.4, 93.5, 113.2, 124.3, 124.5, 126.1, 137.1, 159.8, 161.0; ESI-MS *m/z* 368 [M + Na]⁺. IR (KBr) ν 3308, 2983, 1674, 1600, 1410, 754 cm⁻¹.

Ethyl 3-iodo-5-methoxy-1-methyl-1H-indole-2-carboxylate (**14**)

Compound **11** (1.0 g, 2.9 mmol) was added to a stirred suspension of oil-free sodium hydride NaH (0.1 g, 4.36 mmol) in DMF (10 ml) at 0 °C and the mixture was stirred for 10 min at this temperature. Then methyl iodide (0.49 g, 3.48 mmol) was added at 0 °C and the whole mixture was stirred at room temperature (20 °C) for 1 h. The solution was poured into ice cold water (50 ml) and extracted with CH₂Cl₂ (2 \times 25 ml). The organic layers were dried with sodium sulphate and concentrated under reduced pressure to give **14** in a quantitative yield (1.0 g). ¹H NMR (CDCl₃, 400 MHz) 1.24 (t, *J* = 7.2 Hz, 3H), 3.95 (s, 3H), 3.81 (s, 3H), 4.28 (q, *J* = 7.2 Hz, 2H), 7.23 (d, *J* = 7.4 Hz, 1H), 7.26 (d, *J* = 7.4 Hz, 1H), 7.64 (s, 1H). ¹³C NMR (CDCl₃, 125 MHz) 14.6, 33.6, 55.9, 61.5, 66.5, 103.2, 113.2, 117.9, 129.2, 130.4, 134.5, 155.6, 161.1; ESI-MS *m/z* 360 [M + H]⁺; IR (KBr) ν 2995, 2826, 1701, 1573–1454, 767 cm⁻¹.

General Procedure B: synthesis of 2-nitrophenyl boronic acids (**15–20**)

A dry nitrogen-flushed 25-ml round-bottomed flask equipped with a magnetic stirrer and a septum was loaded with aryl iodide (4.0 mmol, 1.0 equiv.). Dry THF (6 ml) was added, and the resulting solution was cooled to –78 °C. To the resulting cooled mixture was added dropwise 2.2 ml of a 2 M solution of PhMgCl (4.8 mmol, 1.2 equiv.) in THF. After 5 min, 0.536 ml of trimethyl borate (4.8 mmol, 1.2 equiv.) was added dropwise to the reaction solution. The reaction mixture was stirred for 30 min at –78 °C, warmed to –10 °C and quenched with 4 ml of a 2 M aqueous solution of HCl. The resulting mixture was extracted with Et₂O (20 ml) and washed with H₂O (10 ml) and brine (10 ml). The resulting organic layer was dried over Na₂SO₄, filtered, and concentrated under reduced pressure. The crude boronic acids were used in subsequent transformations without additional purification.

General Procedure C: synthesis of 2-nitrophenyl boronic esters (**21–24**)

In a 250-ml round-bottomed flask purged and maintained with an inert atmosphere of nitrogen was placed a solution of substituted-1-bromo-2-nitrobenzene (1.0 equiv.) in 1,4-dioxane (150 ml). Bis(pinacolato)diboron (1.5 equiv.), Pd(dppf)Cl₂ (0.03 equiv.), and potassium acetate (2.0 equiv.) were then added under vigorous stirring and placed in a heated bath at 80 °C. The resulting solution was stirred overnight, cooled to room temperature and concentrated under reduced pressure. The residue was used for further steps without purification.

General procedure D: synthesis of 3-arylated indoles (**25–44**)

To a mixture of ethyl 3-iodo-5- or 6-substituted-1H-Indole-2-carboxylate **10–14** (1.0 equiv.), crude substituted-2-nitroarylboronic acid **15–20** or 4,4,5,5-tetramethyl-2-(substituted-2-nitrophenyl)-1,3,2-dioxaborolane **21–24** (2.0 equiv.) and finally sodium bicarbonate (3.0 equiv.) was added a 10:1 v/v mixture of 1,4-dioxane and water. The reaction mixture was degassed with argon for about 30 min and Pd(PPh₃)₄ (10.0 mol %) was added in one portion. The resulting mixture was heated to 100 °C. After 12 h, the mixture was cooled to room temperature and diluted with cold water. The mixture was extracted with EtOAc. The combined organic layers were washed with brine, dried over Na₂SO₄, filtered and

concentrated *in vacuo*. The crude product was finally purified by silica gel flash chromatography to afford the desired product **25–44**.

Ethyl 3-(2-nitrophenyl)-1H-indole-2-carboxylate (25)

The reaction was carried out as described in general procedure D using **4** (0.100 g, 0.39 mmol, 1.0 equiv.), 1-naphthaleneboronic acid (0.083 g, 0.47 mmol, 1.2 equiv.). Purification by silica gel flash chromatography (EtOAc) afforded **25** (0.083 g, 70%) as a white solid. R_f (EtOAc): 0.17. m.p. 144–146 °C. ^1H NMR (CDCl_3 , 400 MHz) 1.13 (t, $J=7.2$ Hz, 3H), 4.19 (q, $J=7.2$ Hz, 2H), 7.16 (t, $J=7.2$ Hz, 7.6 Hz, 1H), 7.37 (t, $J=8.0$ Hz, 7.2 Hz, 1H), 7.42–7.48 (m, 2H), 7.51–7.56 (m, 2H), 7.67 (t, $J=7.2$ Hz, 7.6 Hz, 1H), 8.10 (d, $J=8.0$ Hz, 1H), 9.14 (s, 1H). ^{13}C NMR ($\text{DMSO}-d_6$, 125 MHz) 13.7, 61.2, 112.0, 118.7, 120.8, 121.3, 123.1, 124.4, 126.0, 127.5, 128.3, 129.2, 132.2, 133.2, 135.7, 150.0, 161.3. ESI-MS m/z 311 $[\text{M} + \text{H}]^+$. IR (KBr) ν 3320, 3001, 2983, 2938, 1693, 1623, 1525, 1433, 1291, 1205, 1117, 784 cm^{-1} .

Ethyl 3-(5-methoxy-2-nitrophenyl)-1H-indole-2-carboxylate (26)

The reaction was carried out as described in general procedure D using **10** (0.100 g, 0.317 mmol, 1.0 equiv.) and (5-methoxy-2-nitrophenyl)boronic acid **17** (0.124 g, 0.634 mmol, 2.0 equiv.). Purification by flash chromatography on silica gel (eluent 9/1 PE/EtOAc) afforded **26** (0.072 g, 67%) as a yellow solid. $R_f = 0.4$ (PE/EtOAc 8/2). ^1H NMR (CDCl_3 , 400 MHz) 1.18 (t, $J=7.2$ Hz, 3H), 3.92 (s, 3H), 4.19–4.24 (m, $J=7.2$ Hz, 2H), 6.98 (d, $J=2.4$ Hz, 1H), 7.02 (dd, $J=2.4$ Hz, 8.8 Hz, 1H), 7.19 (t, $J=7.6$ Hz, 1H), 7.40 (t, $J=7.6$ Hz, 1H), 7.50 (m, 2H), 8.20 (d, $J=8.8$ Hz, 1H), 9.11 (s, 1H); ^{13}C NMR ($\text{DMSO}-d_6$, 125 MHz) 14.4, 55.8, 60.5, 111.9, 112.9, 113.4, 116.9, 117.9, 118.4, 120.6, 121.3, 124.6, 125.1, 127.6, 136.5, 151.6; 153.0, 159.8, 162.0. ESI-MS m/z 341 $[\text{M} + \text{H}]^+$. IR (KBr) ν 3260, 3050, 2958, 1710, 1612, 1507, 1463, 1291, 1167, 1048, 984, 748 cm^{-1} .

Ethyl 3-(4-hydroxy-2-nitrophenyl)-1H-indole-2-carboxylate (27)

The reaction was carried out as described in general procedure using **10** (0.100 g, 0.317 mmol, 1.0 equiv.) and 3-nitro-4-(4,4,5,5-tetramethyl-1,3,2-dioxaborolan-2-yl)phenol **21** (0.168 g, 0.634 mmol, 2.0 equiv.). Purification by flash chromatography on silica gel (eluent 8.5/1.5 PE/EtOAc) afforded **27** (0.052 g, 51%) as a yellow solid. $R_f = 0.3$ (PE/EtOAc 8/2). ^1H NMR (CDCl_3 , 400 MHz) 1.10 (t, $J=6.8$ Hz, 3H), 4.14 (q, $J=6.8$ Hz, 2H), 7.08 (t, $J=7.6$ Hz, 1H), 7.18 (d, $J=7.6$ Hz, 1H), 7.30–7.37 (m, 3H), 7.46 (s, 1H), 7.51 (d, $J=10.5$ Hz, 1H), 10.47 (s, 1H), 11.98 (s, 1H). ^{13}C NMR ($\text{DMSO}-d_6$, 125 MHz) 14.2, 60.9, 111.1, 113.2, 118.3, 119.4, 120.4, 120.6, 121.0, 123.4, 125.6, 127.4, 134.6, 136.8, 150.5, 157.7, 161.5. ESI-MS m/z 327 $[\text{M} + \text{H}]^+$. IR (KBr) ν 3425, 3214, 3049, 2932, 1692, 1620, 1512, 1117, 1026, 984 cm^{-1} .

Ethyl 3-(5-hydroxy-2-nitrophenyl)-1H-indole-2-carboxylate (28)

The reaction was carried out as described in general procedure C using **10** (0.100 g, 0.317 mmol, 1.0 equiv.) and 4-nitro-3-(4,4,5,5-tetramethyl-1,3,2-dioxaborolan-2-yl)phenol **22** (0.168 g, 0.634 mmol, 2.0 equiv.). Purification by flash chromatography on silica gel (eluent 8.5/1.5 PE/EtOAc) afforded **28** (0.058 g, 55%) as a yellow solid. $R_f = 0.3$ (PE/EtOAc 8/2). ^1H NMR (CDCl_3 , 400 MHz) 1.01 (t, $J=7.2$ Hz, 3H), 4.11 (q, $J=7.2$ Hz, 2H), 6.81 (s, 1H), 6.95–6.99 (m, 1H), 7.08–7.11 (m, 1H), 7.29–7.34 (m, 2H), 7.51 (d, $J=8.4$ Hz, 1H), 8.07 (d, $J=8.8$ Hz, 1H), 10.89 (s, 1H, br), 12.04 (s, 1H). ^{13}C NMR ($\text{DMSO}-d_6$, 125 MHz) 14.1, 60.9, 111.8, 113.2, 115.2, 118.7, 119.7, 121.2, 122.8, 123.2, 123.7, 125.6, 127.8, 132.3, 136.8, 141.7, 161.9. ESI-MS m/z 327

$[\text{M} + \text{H}]^+$. IR (KBr) ν 3359, 3245, 3055, 2986, 2939, 1689, 1622, 1518, 1248, 1110, 1060, 975, 734 cm^{-1} .

Ethyl 5-methoxy-3-(2-nitrophenyl)-1H-indole-2-carboxylate (29)

The reaction was carried out as described in general procedure C using **11** (0.100 g, 0.290 mmol, 1.0 equiv.) and (2-nitrophenyl)boronic acid **15** (0.115 g, 0.579 mmol, 2.0 equiv.) and NaHCO_3 (0.073 g, 0.870 mmol, 3.0 equiv.). Purification by flash chromatography on silica gel (eluent 9/1 PE/EtOAc) afforded **29** (0.055 g, 56%) as a yellow solid. $R_f = 0.4$ (PE/EtOAc 8/2). ^1H NMR (CDCl_3 , 400 MHz) 1.12 (t, $J=7.2$ Hz, 3H), 3.76 (s, 3H), 4.17 (q, $J=7.2$ Hz, 2H), 6.76 (d, $J=2.4$ Hz, 1H), 7.04 (dd, $J=2.4$ Hz, 8.8 Hz, 1H), 7.35 (d, $J=9.2$ Hz, 1H), 7.52–7.56 (m, 2H), 7.67 (t, $J=7.2$ Hz, 1H), 8.08 (d, $J=8.0$ Hz, 1H), 9.01 (s, 1H). ^{13}C NMR ($\text{DMSO}-d_6$, 125 MHz) 14.1, 55.7, 60.9, 100.1, 114.4, 117.4, 117.5, 123.7, 124.7, 127.3, 129.0, 129.4, 132.1, 133.3, 133.7, 150.2, 155.0, 161.3. ESI-MS m/z 341 $[\text{M} + \text{H}]^+$. IR (KBr) ν 3245, 3060, 2974, 2918, 1698, 1608, 1520, 1404, 1117, 1023, 984, 735 cm^{-1} .

Ethyl 5-methoxy-3-(4-methoxy-2-nitrophenyl)-1H-indole-2-carboxylate (30)

The reaction was carried out as described in general procedure C using **11** (0.100 g, 0.290 mmol, 1.0 equiv.) and (4-methoxy-2-nitrophenyl)boronic acid **16** (0.113 g, 0.579 mmol, 2.0 equiv.). Purification by flash chromatography on silica gel (eluent 8/2 PE/EtOAc) afforded **30** (0.043 g, 40%) as a yellow solid. $R_f = 0.35$ (PE/EtOAc 8/2). ^1H NMR (CDCl_3 , 400 MHz) 1.17 (t, $J=7.2$ Hz, 3H), 3.76 (s, 3H), 3.94 (s, 3H), 4–19 (q, $J=7.2$ Hz, 2H), 6.77 (d, $J=2.4$ Hz, 1H), 7.03 (dd, $J=2.4$ Hz, 8.8 Hz, 1H), 7.21 (dd, $J=2.8$ Hz, 8.4 Hz, 1H), 7.34 (d, $J=8.8$ Hz, 1H), 7.42 (d, $J=8.4$ Hz, 1H), 7.63 (d, $J=2.8$ Hz, 1H), 9.01 (s, 1H). ^{13}C NMR ($\text{DMSO}-d_6$, 125 MHz) 14.1, 55.7, 56.5, 60.9, 100.1, 109.8, 114.4, 117.3, 119.3, 121.2, 123.7, 123.8, 127.6, 132.1, 134.6, 150.8, 155.0, 159.2, 161.4. ESI-MS m/z 371 $[\text{M} + \text{H}]^+$. IR (KBr) ν 3254, 3030, 2934, 1703, 1613, 1556, 1403, 1209, 1017, 980, 756 cm^{-1} .

Ethyl 5-methoxy-3-(5-methoxy-2-nitrophenyl)-1H-indole-2-carboxylate (31)

The reaction was carried out as described in general procedure C using **11** (0.100 g, 0.290 mmol, 1.0 equiv.) and (5-methoxy-2-nitrophenyl)boronic acid **17** (0.113 g, 0.579 mmol, 2.0 equiv.). Purification by flash chromatography on silica gel (eluent 8/2 PE/EtOAc) afforded **31** (0.053 g, 49%) as a yellow solid. $R_f = 0.35$ (PE/EtOAc 8/2). ^1H NMR (CDCl_3 , 400 MHz) 1.19 (t, $J=7.2$ Hz, 3H), 3.79 (s, 3H), 3.97 (s, 3H), 4.22 (q, $J=7.2$ Hz, 2H), 6.80 (d, $J=2.4$ Hz, 1H), 7.05 (dd, $J=2.4$ Hz, 8.4 Hz, 1H), 7.24 (dd, $J=2.4$ Hz, 8.8 Hz, 1H), 7.36 (d, $J=8.8$ Hz, 1H), 7.45 (d, $J=8.4$ Hz, 1H), 7.65 (d, $J=2.4$ Hz, 1H), 9.12 (s, 1H). ^{13}C NMR ($\text{DMSO}-d_6$, 125 MHz) 14.1, 55.7, 56.8, 60.9, 100.2, 114.0, 114.5, 116.7, 117.3, 118.3, 123.6, 127.2, 127.8, 132.3, 137.5, 140.1, 155.0, 161.3, 163.8. ESI-MS m/z 371 $[\text{M} + \text{H}]^+$. IR (KBr) ν 3320, 3001, 2983, 2938, 1673, 1623, 1525, 1433, 1291, 1117, 984 cm^{-1} .

Ethyl 3-(4,5-dimethoxy-2-nitrophenyl)-5-methoxy-1H-indole-2-carboxylate (32)

The reaction was carried out as described in general procedure C using **11** (0.100 g, 0.290 mmol, 1.0 equiv.) and (4,5-dimethoxy-2-nitrophenyl)boronic acid **18** (0.131 g, 0.579 mmol, 2.0 equiv.). Purification by flash chromatography on silica gel (eluent 8/2 PE/EtOAc) afforded **32** (0.064 g, 55%) as a yellow solid, which was

used in the next step. ^1H NMR (CDCl_3 , 400 MHz) 1.17 (t, $J=7.2$ Hz, 3H), 3.77 (s, 3H), 3.93 (s, 3H), 4.03 (s, 3H), 4.20 (q, $J=7.2$ Hz, 2H), 6.77 (d, $J=2.0$ Hz, 1H), 6.90 (s, 1H), 7.05 (dd, $J=2.0$ Hz, 8.8 Hz, 1H), 7.36 (d, $J=8.8$ Hz, 1H), 7.75 (s, 1H), 8.95 (s, 1H). ESI-MS m/z 401 $[\text{M} + \text{H}]^+$. IR (KBr) ν 3070, 2980, 2930, 1705, 1633, 1525, 1433, 1291, 1132, 1045, 984 cm^{-1} .

Ethyl 5-methoxy-3-(2-nitro-5-(trifluoromethyl)phenyl)-1H-indole-2-carboxylate (33)

The reaction was carried out as described in general procedure C using **11** (0.100 g, 0.290 mmol, 1.0 equiv.) and (2-nitro-5-(trifluoromethyl)phenyl)boronic acid **19** (0.136 g, 0.579 mmol, 2.0 equiv.). Purification by flash chromatography on silica gel (eluent 8/2 PE/EtOAc) afforded **33** (0.055 g, 47%) as a yellow solid. ^1H NMR (CDCl_3 , 400 MHz) 1.17 (t, $J=7.2$ Hz, 3H), 3.80 (s, 3H), 4.21–4.26 (m, $J=7.2$ Hz, 2H), 6.76 (d, $J=2.0$ Hz, 1H), 7.09 (dd, $J=2.0$ Hz, 8.8 Hz, 1H), 7.39 (d, $J=8.8$ Hz, 1H), 7.84 (d, $J=8.4$ Hz, 1H), 7.87 (s, 1H), 8.19 (d, $J=8.4$ Hz, 1H), 9.17 (s, 1H). ^{13}C NMR ($\text{DMSO}-d_6$, 125 MHz) 14.0, 55.7, 61.1, 99.9, 114.5, 115.4, 117.5, 122.3, 124.3, 125.8, 126.3, 127.1, 130.4, 131.0, 132.0, 132.8, 152.4, 155.2, 161.1. ESI-MS m/z 409 $[\text{M} + \text{H}]^+$. IR (KBr) ν 3290, 3071, 2929, 1685, 1622, 1200, 1098, 978, 756 cm^{-1} .

Ethyl 3-(4-hydroxy-2-nitrophenyl)-5-methoxy-1H-indole-2-carboxylate (34)

The reaction was carried out as described in general procedure C using **11** (0.100 g, 0.290 mmol, 1.0 equiv.) and 3-nitro-4-(4,4,5,5-tetramethyl-1,3,2-dioxaborolan-2-yl)phenol **21** (0.153 g, 0.579 mmol, 2.0 equiv.) and NaHCO_3 (0.073 g, 0.870 mmol, 3.0 equiv.). Purification by flash chromatography on silica gel (eluent 8/2 PE/EtOAc) afforded **34** (0.046 g, 45%) as a yellow solid, which was used in the next step. $R_f = 0.3$ (PE/EtOAc 8/2). ^1H NMR (CDCl_3 , 400 MHz) 1.10 (t, $J=6.8$ Hz, 3H), 3.68 (s, 3H), 4.10 (q, $J=6.8$ Hz, 2H), 6.68 (d, $J=2.4$ Hz, 1H), 6.98 (dd, $J=2.4$ Hz, 8.8 Hz, 1H), 7.18 (dd, $J=2.4$ Hz, 8.4 Hz, 1H), 7.36–7.42 (m, 2H), 7.44 (d, $J=2.4$ Hz, 1H), 10.45 (s, 1H), 11.86 (s, 1H). ESI-MS m/z 357 $[\text{M} + \text{H}]^+$; IR (KBr) ν 3405, 3344, 3074, 2966, 2918, 1690, 1623, 1505, 1433, 1210, 1117, 1054, 764 cm^{-1} .

Ethyl 3-(5-hydroxy-2-nitrophenyl)-5-methoxy-1H-indole-2-carboxylate (35)

The reaction was carried out as described in general procedure C using **11** (0.100 g, 0.290 mmol, 1.0 equiv.) and 4-nitro-3-(4,4,5,5-tetramethyl-1,3,2-dioxaborolan-2-yl)phenol **22** (0.153 g, 0.579 mmol, 2.0 equiv.). Purification by flash chromatography on silica gel (eluent 8/2 PE/EtOAc) afforded **35** (0.044 g, 43%) as a yellow solid. $R_f = 0.3$ (PE/EtOAc 8/2). ^1H NMR (CDCl_3 , 400 MHz) 1.09 (t, $J=7.2$ Hz, 3H), 3.69 (s, 3H), 4.10 (q, $J=7.2$ Hz, 2H), 6.70 (d, $J=2.0$ Hz, 1H), 6.81 (d, $J=2.8$ Hz, 1H), 6.94–7.00 (m, 2H), 7.42 (d, $J=8.8$ Hz, 1H), 8.07 (d, $J=8.8$ Hz, 1H), 10.83 (s, br, 1H), 11.93 (s, 1H). ^{13}C NMR ($\text{DMSO}-d_6$, 125 MHz) 14.1, 55.7, 60.8, 100.2, 114.3, 115.1, 117.2, 118.2, 119.6, 123.5, 127.1, 127.8, 132.1, 132.5, 141.8, 154.9, 161.3, 161.9. ESI-MS m/z 357 $[\text{M} + \text{H}]^+$. IR (KBr) ν 3438, 3247, 3060, 2970, 2920, 1694, 1620, 1535, 1420, 1249, 1145, 1057, $984, 734\text{ cm}^{-1}$.

Ethyl 3-(5-amino-2-nitrophenyl)-5-methoxy-1H-indole-2-carboxylate (36)

The reaction was carried out as described in general procedure C using **11** (0.100 g, 0.290 mmol, 1.0 equiv.) and 4-nitro-3-(4,4,5,5-

tetramethyl-1,3,2-dioxaborolan-2-yl)aniline **23** (0.153 g, 0.579 mmol, 2.0 equiv.). Purification by flash chromatography on silica gel (eluent 8/2 PE/EtOAc) afforded **36** (0.041 g, 40%) as a yellow solid, which was used in the next step. $R_f = 0.3$ (PE/EtOAc 8/2). ^1H NMR (CDCl_3 , 400 MHz) 1.14 (t, $J=7.2$ Hz, 3H), 3.76 (s, 3H), 4.14 (q, $J=7.2$ Hz, 2H), 5.38 (s, 2H), 6.62 (d, $J=2.4$ Hz, 1H), 6.68 (dd, $J=2.4$ Hz, 8.8 Hz, 1H), 6.78 (d, $J=2.4$ Hz, 1H), 6.95 (dd, $J=2.4$ Hz, 8.8 Hz, 1H), 7.41 (d, $J=8.8$ Hz, 1H), 8.03 (d, $J=8.8$ Hz, 1H), 11.05 (s, 1H). ESI-MS m/z 356 $[\text{M} + \text{H}]^+$. IR (KBr) ν 3400–3200 (br.), 3014, 2912, 1682, 1618, 1514, 1402, 1102, 1009, 980, 745 cm^{-1} .

Ethyl 3-(5-acetamido-2-nitrophenyl)-5-methoxy-1H-indole-2-carboxylate (37)

The reaction was carried out as described in general procedure C using **11** (0.100 g, 0.290 mmol, 1.0 equiv.) and *N*-(4-nitro-3-(4,4,5,5-tetramethyl-1,3,2-dioxaborolan-2-yl)phenyl) acetamide **24** (0.177 g, 0.579 mmol, 2.0 equiv.). Purification by flash chromatography on silica gel (eluent 9/1 PE/EtOAc) afforded **37** (0.063 g, 55%) as a yellow solid. $R_f = 0.4$ (PE/EtOAc 8/2). ^1H NMR (CDCl_3 , 400 MHz) 1.06 (t, $J=6.8$ Hz, 3H), 2.09 (s, 3H), 3.68 (s, 3H), 4.05–4.11 (m, $J=6.8$, 2H), 6.74 (d, $J=2.4$ Hz, 1H), 6.99 (dd, $J=2.4$ Hz, 9.2 Hz, 1H), 7.42 (d, $J=9.2$ Hz, 1H), 7.74 (d, $J=2.0$ Hz, 1H), 7.79 (dd, $J=2.0$ Hz, 9.2 Hz, 1H), 8.12 (d, $J=9.2$ Hz, 1H), 10.45 (s, 1H), 11.95 (s, 1H). ^{13}C NMR ($\text{DMSO}-d_6$, 125 MHz) δ 14.2, 24.8, 55.8, 60.9, 100.3, 114.4, 117.3, 117.8, 118.0, 122.7, 123.6, 126.6, 127.1, 131.0, 132.1, 143.7, 144.2, 155.0, 161.3, 169.8. ESI-MS m/z 398 $[\text{M} + \text{H}]^+$. IR (KBr) ν 3352, 3301, 3117, 3057, 2986, 2938, 1710, 1698, 1621, 1405, 1264, 1118, 1034, 973, 763 cm^{-1} .

Ethyl 6-methoxy-3-(2-nitrophenyl)-1H-indole-2-carboxylate (38)

The reaction was carried out as described in general procedure C using **12** (0.100 g, 0.290 mmol, 1.0 equiv.) and (2-nitrophenyl)boronic acid **15** (0.115 g, 0.579 mmol, 2.0 equiv.). Purification by flash chromatography on silica gel (eluent 9/1 PE/EtOAc) afforded **38** (0.052 g, 53%) as a yellow solid. $R_f = 0.4$ (PE/EtOAc 8/2). ^1H NMR (CDCl_3 , 400 MHz) 1.10 (t, $J=7.2$ Hz, 3H), 3.85 (s, 3H), 4.15 (q, $J=7.2$ Hz, 2H), 6.81 (dd, $J=2.4$, 8.8 Hz, 1H), 6.85 (d, $J=1.6$ Hz, 1H), 7.28 (d, $J=8.8$ Hz, 1H), 7.48–7.54 (m, 2H), 7.62–7.66 (m, 1H), 8.06 (dd, $J=0.8$, 8.8 Hz, 1H), 9.07 (s, 1H). ^{13}C NMR ($\text{DMSO}-d_6$, 125 MHz) 14.1, 55.7, 60.7, 94.5, 113.0, 118.4, 121.4, 121.6, 122.2, 124.6, 129.1, 133.2, 133.6, 137.9, 150.2, 158.8, 161.3. ESI-MS m/z 341 $[\text{M} + \text{H}]^+$. IR (KBr) ν 3350, 3050, 2918, 1706, 1620, 1555, 1450, 1279, 1133, 1043, 984, 732 cm^{-1} .

Ethyl 6-methoxy-3-(5-methoxy-2-nitrophenyl)-1H-indole-2-carboxylate (39)

The reaction was carried out as described in general procedure C using **12** (0.100 g, 0.290 mmol, 1.0 equiv.) and (5-methoxy-2-nitrophenyl)boronic acid **17** (0.113 g, 0.579 mmol, 2.0 equiv.). Purification by flash chromatography on silica gel (eluent 8/2 PE/EtOAc) afforded **39** (0.062 g, 58%) as a yellow solid. $R_f = 0.35$ (PE/EtOAc 8/2). ^1H NMR (CDCl_3 , 400 MHz) 1.13 (t, $J=7.2$ Hz, 3H), 3.86 (s, 3H), 3.88 (s, 3H), 4.15 (q, $J=7.2$ Hz, 2H), 6.82 (d, $J=8.4$ Hz, 1H), 6.86 (s, 1H), 6.93 (s, 1H), 6.98 (d, $J=9.2$ Hz, 1H), 7.32 (d, $J=8.4$ Hz, 1H), 8.15 (d, $J=9.2$ Hz, 1H), 7.32 (d, $J=8.4$ Hz, 1H), 8.15 (d, $J=9.2$ Hz, 1H), 9.0 (s, 1H). ^{13}C NMR ($\text{DMSO}-d_6$, 125 MHz) 14.2, 55.8, 56.6, 60.8, 94.6, 113.0, 113.9, 116.7, 118.5, 121.5, 122.1, 127.4, 132.2, 137.9, 140.0, 143, 158.9, 161.4, 162.7. ESI-MS m/z 371 $[\text{M} + \text{H}]^+$. IR (KBr) ν 3040, 2948, 1710, 1615, 1534, 1450, 1273, 1047, 990, 734 cm^{-1} .

Ethyl 5-fluoro-3-(5-methoxy-2-nitrophenyl)-1H-indole-2-carboxylate (40)

The reaction was carried out as described in general procedure C using **13** (0.100 g, 0.300 mmol, 1.0 equiv.) and (5-methoxy-2-nitrophenyl)boronic acid **17** (0.118 g, 0.600 mmol, 2.0 equiv.). Purification by flash chromatography on silica gel (eluent 9/1 PE/EtOAc) afforded **40** (0.066 g, 61%) as a yellow solid, which was used in the next step. $R_f = 0.4$ (PE/EtOAc 8/2). ^1H NMR (CDCl_3 , 400 MHz) 1.17 (t, $J = 7.2$ Hz, 3H), 3.92 (s, 3H), 4.21 (q, $J = 7.2$ Hz, 2H), 6.94 (d, $J = 2.4$ Hz, 1H), 8.20 (d, $J = 9.2$ Hz, 1H), 7.44 (dd, $J = 2.4$ Hz, 9.2 Hz, 1H), 7.10–7.19 (m, 3H). ESI-MS m/z 359 $[\text{M} + \text{H}]^+$. IR (KBr) ν 3205, 3092, 2952, 2914, 1698, 1623, 1525, 1405, 1273, 1176, 1047, 936, 724 cm^{-1} .

Ethyl 5-fluoro-3-(5-hydroxy-2-nitrophenyl)-1H-indole-2-carboxylate (41)

The reaction was carried out as described in general procedure C using **13** (0.100 g, 0.300 mmol, 1.0 equiv.) and 4-nitro-3-(4,4,5,5-tetramethyl-1,3,2-dioxaborolan-2-yl)phenol **22** (0.159 g, 0.600 mmol, 2.0 equiv.). Purification by flash chromatography on silica gel (eluent 8/2 PE/EtOAc) afforded **41** (0.053 g, 52%) as a yellow solid. $R_f = 0.3$ (PE/EtOAc 8/2). ^1H NMR (CDCl_3 , 400 MHz) 1.17 (t, $J = 6.8$ Hz, 3H), 4.20 (q, $J = 6.8$ Hz, 2H), 6.81 (s, 1H), 7.00 (d, $J = 6.8$ Hz, 1H), 7.06 (d, $J = 8.0$ Hz, 1H), 7.21 (t, $J = 6.8$ Hz, 1H), 7.53 (s, 1H), 8.09 (d, $J = 7.6$ Hz, 1H), 10.88 (s, 1H), 12.19 (s, br, 1H). ^{13}C NMR ($\text{DMSO}-d_6$, 125 MHz) 14.1, 61.1, 104.8, 114.8, 115.3, 119.6, 124.9, 126.7, 127.01, 127.9, 131.8, 133.5, 141.5, 156.9, 159.3, 161.1, 162.0. ESI-MS m/z 345 $[\text{M} + \text{H}]^+$. IR (KBr) ν 3412, 3150, 3052, 2908, 1704, 1623, 1565, 1453, 1271, 1137, 1043, 984, 734 cm^{-1} .

Ethyl 3-(5-hydroxy-2-nitrophenyl)-5-methoxy-1-methyl-1H-indole-2-carboxylate (42)

The reaction was carried out as described in general procedure C using **14** (0.100 g, 0.278 mmol, 1.0 equiv.) and 4-nitro-3-(4,4,5,5-tetramethyl-1,3,2-dioxaborolan-2-yl)phenol **22** (0.148 g, 0.557 mmol, 2.0 equiv.) and NaHCO_3 (0.070 g, 0.834 mmol, 3.0 equiv.). Purification by flash chromatography on silica gel (eluent 9/1 PE/EtOAc) afforded **42** (0.065 g, 63%) as a yellow solid. $R_f = 0.4$ (PE/EtOAc 9/1). ^1H NMR (CDCl_3 , 400 MHz) 1.04 (t, $J = 7.2$ Hz, 3H), 3.79 (s, 3H), 4.06 (s, 3H), 4.12 (q, $J = 7.2$ Hz, 2H), 6.31 (s, 1H, br), 6.72 (dd, $J = 8.2$ Hz, 1.4 Hz, 1H), 6.77 (dd, $J = 7.6$ Hz, 2.1 Hz, 1H), 6.92 (d, $J = 7.6$ Hz, 1H), 6.95 (d, $J = 8.2$ Hz, 1H), 7.14 (d, $J = 1.4$ Hz, 1H), 7.75 (d, $J = 2.1$ Hz, 1H). ^{13}C NMR ($\text{DMSO}-d_6$, 125 MHz) 13.8, 32.7, 55.8, 60.8, 100.5, 112.9, 115.2, 117.3, 119.5, 124.6, 125.9, 126.0, 127.8, 133.1, 134.2, 141.7, 155.2, 161.5, 162.0. ESI-MS m/z 371 $[\text{M} + \text{H}]^+$. IR (KBr) ν 3040, 2948, 1710, 1615, 1534, 1450, 1273, 1047, 990, 734 cm^{-1} .

Ethyl 5-methoxy-1-methyl-3-(2-nitro-5-(trifluoromethyl)phenyl)-1H-indole-2-carboxylate (43)

The reaction was carried out as described in general procedure C using **14** (0.100 g, 0.278 mmol, 1.0 equiv.) and (2-nitro-5-(trifluoromethyl)phenyl)boronic acid **19** (0.131 g, 0.557 mmol, 2.0 equiv.). Purification by flash chromatography on silica gel (eluent 9/1 PE/EtOAc) afforded **43** (0.063 g, 54%) as a yellow solid. $R_f = 0.4$ (PE/EtOAc 8/2). ^1H NMR (CDCl_3 , 400 MHz) 0.99 (t, $J = 6.8$ Hz, 3H), 3.78 (s, 3H), 4.09–4.16 (m, 5H, $\text{N}-\text{CH}_3$ and CH_2), 6.68 (dd, $J = 2.4$ Hz, 10.8 Hz, 1H), 7.11 (dd, $J = 2.4$ Hz, 8.8 Hz, 1H), 7.38 (d, $J = 8.8$ Hz, 1H), 7.79 (s, 1H), 7.82 (d, $J = 8.4$ Hz, 1H), 8.15 (d, $J = 8.4$ Hz, 1H). ^{13}C NMR ($\text{DMSO}-d_6$, 125 MHz) 13.6, 32.9, 55.8, 61.0, 100.2, 113.1, 116.5, 117.6, 125.2, 125.6, 125.9, 126.1, 126.4, 130.8, 130.9, 134.1, 152.5,

155.4, 155.5, 161.1. ESI-MS m/z 423 $[\text{M} + \text{H}]^+$. IR (KBr) ν 3051, 2959, 2912, 1689, 1616, 1409, 1104, 1012, 979, 746 cm^{-1} .

Ethyl 3-(5-(dimethylamino)-2-nitrophenyl)-5-methoxy-1-methyl-1H-indole-2-carboxylate (44)

The reaction was carried out as described in general procedure C using **14** (0.100 g, 0.278 mmol, 1.0 equiv.) and (2-(dimethylamino)-5-nitrophenyl)boronic acid **20** (0.117 g, 0.557 mmol, 2.0 equiv.). Purification by flash chromatography on silica gel (eluent 9/1 PE/EtOAc) afforded **44** (0.072 g, 65%) as a yellow solid, which was used in the next step. $R_f = 0.5$ (PE/EtOAc 8/2). ^1H NMR (CDCl_3 , 400 MHz) 1.00 (t, $J = 7.2$ Hz, 3H), 3.07 (s, 6H), 3.75 (s, 3H), 4.05–4.11 (m, 5H), 6.55 (d, $J = 2.8$ Hz, 1H), 6.66 (dd, $J = 2.8$ Hz, 9.2 Hz, 1H), 6.76 (d, $J = 2.4$ Hz, 1H), 7.05 (dd, $J = 2.4$ Hz, 8.8 Hz, 1H), 7.33 (d, $J = 8.8$ Hz, 1H), 8.19 (d, $J = 9.2$ Hz, 1H). ESI-MS m/z 398 $[\text{M} + \text{H}]^+$. IR (KBr) ν 3045, 2980, 2928, 1701, 1612, 1515, 1403, 1241, 1107, 1032, 975, 729 cm^{-1} .

General procedure D: synthesis of the indolo[2,3-c]quinolin-6-one library 45–64

Ethyl 3-(substituted-2-nitrophenyl)-1H-substituted-indole-2-carboxylate **25–44** (1.0 equiv.) was dissolved in acetic acid and Iron (Fe) powder (5.0 equiv.) was added. The reaction mixture was heated to 110 °C for about 12 h. After completion of the reaction, the acetic acid was removed under reduced pressure and the residue was diluted with EtOAc. After filtration and evaporation under reduced pressure, the crude material was purified by silica gel flash chromatography ($\text{CH}_3\text{OH}/\text{CH}_2\text{Cl}_2$).

5,7-Dihydro-6H-indolo[2,3-c]quinolin-6-one (45)

The reaction was carried out as described in general procedure D using **25** (0.090 g, 0.29 mmol, 1.0 equiv.). Purification by flash chromatography on silica gel (eluent 9/1 $\text{CH}_2\text{Cl}_2/\text{MeOH}$) afforded **45** (0.054 g, 80%) as a white solid. $R_f = 0.5$ (5% CH_3OH in CH_2Cl_2). mp 233–237 °C. ^1H NMR ($\text{DMSO}-d_6$, 400 MHz) 7.31–7.36 (m, 2H), 7.42 (d, $J = 7.6$ Hz, 1H), 7.46–7.53 (m, 2H), 7.65 (d, $J = 8$ Hz, 1H), 8.45 (d, $J = 7.6$ Hz, 1H), 8.48 (d, $J = 8.0$ Hz, 1H), 11.87 (s, 1H, imid-NH), 12.37 (s, 1H, amide-NH). ^{13}C NMR ($\text{DMSO}-d_6$, 125 MHz) 113.5, 116.5, 118.5, 118.7, 121.1, 122.7, 122.8, 123.4, 126.1, 126.3, 128.1, 135.4, 139.3, 156.2. ESI-MS m/z 235 $[\text{M} + \text{H}]^+$. HRMS (TOF-MS): m/z calcd for $\text{C}_{15}\text{H}_{11}\text{N}_2\text{O}$ $[\text{M} + \text{H}]^+$: 235.0871, found: 235.0861; IR (KBr) ν 3319, 3157, 3004, 1655, 1621, 1594, 1254, 731 cm^{-1} .

2-Methoxy-5,7-dihydro-6H-indolo[2,3-c]quinolin-6-one (46)

The reaction was carried out as described in general procedure D using **26** (0.070 g, 0.205 mmol, 1.0 equiv.). Purification by flash chromatography on silica gel (eluent 9/1 $\text{CH}_2\text{Cl}_2/\text{MeOH}$) afforded **46** (0.038 g, 70%) as a white solid. $R_f = 0.4$ (5% CH_3OH in CH_2Cl_2). mp >250 °C. ^1H NMR ($\text{DMSO}-d_6$, 400 MHz) 3.94 (s, 3H), 7.07 (dd, $J = 2.4$ Hz, 8.8 Hz, 1H), 7.33 (t, $J = 7.2$ Hz, 7.6 Hz, 1H), 7.45 (d, $J = 8.8$ Hz, 1H), 7.49 (d, $J = 7.6$ Hz, 1H), 7.65 (t, $J = 7.2$ Hz, 8.4 Hz, 1H), 7.80 (d, $J = 2.4$ Hz, 1H), 8.45 (d, $J = 8.4$ Hz, 1H), 11.73 (s, 1H), 12.32 (s, 1H). ^{13}C NMR ($\text{DMSO}-d_6$, 125 MHz) 56.0, 106.1, 113.5, 114.5, 117.7, 118.3, 119.2, 121.1, 122.7, 126.0, 128.5, 129.6, 139.2, 155.3, 155.6. ESI-MS m/z 265 $[\text{M} + \text{H}]^+$. HRMS (TOF-MS): m/z calcd for $\text{C}_{16}\text{H}_{13}\text{N}_2\text{O}_2$ $[\text{M} + \text{H}]^+$: 265.0977, found: 265.0965. m/z calcd for $\text{C}_{15}\text{H}_{10}\text{N}_2\text{O}_2\text{Na}$ $[\text{M} + \text{Na}]^+$: 287.1768, found: 287.1752. IR (KBr) ν 3150, 3041, 2928, 1659, 1601, 1574, 1202, 1137, 1020, 764 cm^{-1} .

3-Hydroxy-5,7-dihydro-6H-indolo[2,3-c]quinolin-6-one (47)

The reaction was carried out as described in general procedure D using **27** (0.050 g, 0.153 mmol, 1.0 equiv). The crude mixture was purified by flash chromatography on silica gel (eluent 9/1 CH₂Cl₂/MeOH) and afforded **47** (0.030 g, 71%) as a white solid. *R_f* = 0.4 (5% CH₃OH in CH₂Cl₂). mp 238–240 °C (decomp.). ¹H NMR (DMSO-*d*₆, 400 MHz) 6.81 (dd, *J* = 2.0 Hz, 8.4 Hz, 1H), 6.92 (d, *J* = 2.0 Hz, 1H), 7.26 (t, *J* = 7.6 Hz, 8.0 Hz, 1H), 7.43 (t, *J* = 7.6 Hz, 8.0 Hz, 1H), 7.59 (d, *J* = 8.0 Hz, 1H), 8.24 (d, *J* = 8.4 Hz, 1H), 8.39 (d, *J* = 8.0 Hz, 1H), 9.73 (s, br, 1H), 11.65 (s, 1H), 12.09 (s, 1H). ¹³C NMR (DMSO-*d*₆, 125 MHz) 101.8, 102.1, 111.1, 119.5, 120.6, 120.7, 122.4, 122.7, 124.5, 125.9, 126.0, 126.2, 137.0, 139.3, 156.4; ESI-MS *m/z* 251 [M + H]⁺. HRMS (TOF-MS): *m/z* calcd for C₁₅H₁₁N₂O₂ [M + H]⁺: 251.0820, found: 251.0810. IR (KBr) ν 3425, 3234, 3135, 3021, 1665, 1610, 1587, 1130, 754 cm⁻¹.

2-Hydroxy-5,7-dihydro-6H-indolo[2,3-c]quinolin-6-one (48)

The reaction was carried out as described in general procedure D using **28** (0.055 g, 0.169 mmol, 1.0 equiv). The crude mixture was purified by flash chromatography on silica gel (eluent 9/1 CH₂Cl₂/MeOH) to afford **48** (0.032 g, 75%) as a white solid. *R_f* = 0.4 (5% CH₃OH in CH₂Cl₂). mp 235–238 °C. ¹H NMR (DMSO-*d*₆, 400 MHz) 6.90 (d, *J* = 8.0 Hz, 1H), 7.28–7.36 (m, *J* = 8.0 Hz, 2H), 7.46 (t, *J* = 7.2 Hz, 6.8 Hz, 1H), 7.64 (d, *J* = 8.0 Hz, 1H), 7.79 (s, 1H), 8.31 (d, *J* = 7.2 Hz, 1H), 10.94 (s, br, 1H), 11.67 (s, 1H), 12.28 (s, 1H). ¹³C NMR (DMSO-*d*₆, 125 MHz) 108.0, 113.5, 115.2, 117.5, 118.3, 119.3, 121.0, 122.2, 122.8, 128.4, 128.5, 139.2, 153.4, 155.5. ESI-MS *m/z* 251 [M + H]⁺. HRMS (TOF-MS): *m/z* calcd for C₁₅H₁₁N₂O₂ [M + H]⁺: 251.0820, found: 251.0815. IR (KBr) ν 3410, 3213, 3150, 3056, 1675, 1611, 1554, 1210, 1130, 784 cm⁻¹.

10-Methoxy-5,7-dihydro-6H-indolo[2,3-c]quinolin-6-one (49)

The reaction was carried out as described in general procedure D using **29** (0.050 g, 0.147 mmol, 1.0 equiv). The crude mixture was purified by flash chromatography on silica gel (eluent 9/1 CH₂Cl₂/MeOH) to afford **49** (0.032 g, 83%) as a white solid. *R_f* = 0.5 (5% CH₃OH in CH₂Cl₂); mp 232–235 °C; ¹H NMR (DMSO-*d*₆, 400 MHz) 3.94 (3H, s, -OCH₃), 7.14 (dd, *J* = 2.0, 6.8 Hz, 1H), 7.36 (t, *J* = 6.8 Hz, 1H), 7.38 (t, *J* = 7.2 Hz, 1H), 7.50 (d, *J* = 7.6 Hz, 1H), 7.54 (d, *J* = 7.6 Hz, 1H), 7.83 (d, *J* = 2.0 Hz, 1H), 8.44 (dd, *J* = 7.2 Hz, 1H); ¹³C NMR (DMSO-*d*₆, 125 MHz) 56.2, 103.8, 114.3, 116.4, 116.9, 118.2, 118.6, 122.7, 122.9, 123.4, 126.1, 128.4, 134.4, 135.2, 154.8, 156.2; ESI-MS *m/z* 265 [M + H]⁺; HRMS (TOF-MS): *m/z* calcd for C₁₆H₁₃N₂O₂ [M + H]⁺: 265.0977, found: 265.0972; IR (KBr) ν 3310, 3135, 3044, 2948, 1660, 1611, 1583, 1204, 1021, 740 cm⁻¹.

3,10-Dimethoxy-5,7-dihydro-6H-indolo[2,3-c]quinolin-6-one (50)

The reaction was carried out as described in general procedure D using **30** (0.040 g, 0.108 mmol, 1.0 equiv). The crude mixture was purified by flash chromatography on silica gel (eluent 9/1 CH₂Cl₂/MeOH) to afford **50** (0.024 g, 75%) as a white solid. *R_f* = 0.5 (5% CH₃OH in CH₂Cl₂); mp 192–195 °C; ¹H NMR (DMSO-*d*₆, 400 MHz) 3.83 (s, 3H), 3.92 (s, 3H), 6.95 (d, *J* = 8.8 Hz, 1H), 7.05 (s, 1H), 7.11 (d, *J* = 8.8 Hz, 1H), 7.51 (d, *J* = 8.8 Hz, 1H), 7.78 (s, 1H), 8.34 (d, *J* = 8.8 Hz, 1H), 11.67 (s, 1H), 12.06 (s, 1H); ¹³C NMR (DMSO-*d*₆, 125 MHz) 55.6, 56.1, 100.3, 103.6, 110.7, 112.4, 114.3, 117.0, 118.8, 122.5, 124.6, 126.9, 134.5, 136.6, 154.6, 156.4, 158.0; ESI-MS *m/z* 295 [M + H]⁺; HRMS (TOF-MS): *m/z* calcd for C₁₇H₁₅N₂O₃ [M + H]⁺: 295.1082, found: 295.1070; IR (KBr) ν 3265, 3105, 3060, 2981, 1668, 1612, 1564, 1210, 1150, 1026, 755 cm⁻¹.

2,10-Dimethoxy-5,7-dihydro-6H-indolo[2,3-c]quinolin-6-one (51)

The reaction was carried out as described in general procedure D using **31** (0.050 g, 0.135 mmol, 1.0 equiv.). The crude mixture was purified by flash chromatography on silica gel (eluent 9/1 CH₂Cl₂/MeOH) to afford **51** (0.027 g, 68%) as a white solid. *R_f* = 0.5 (5% CH₃OH in CH₂Cl₂). mp 190–192 °C. ¹H NMR (DMSO-*d*₆, 400 MHz) 3.93 (s, 6H), 7.06 (dd, *J* = 2.0 Hz, 8.8 Hz, 1H), 7.14 (dd, *J* = 2.0 Hz, 7.2 Hz, 1H), 7.42 (d, *J* = 8.8 Hz, 1H), 7.65 (d, *J* = 8.8 Hz, 1H), 7.75 (s, 2H), 11.70 (s, 1H, NH), 12.23 (s, 1H, NH). ¹³C NMR (DMSO-*d*₆, 125 MHz) 55.7, 56.0, 95.2, 105.8, 112.1, 114.7, 116.8, 117.7, 118.9, 119.0, 123.7, 127.7, 129.8, 140.7, 155.2, 155.4, 158.8. ESI-MS *m/z* 295 [M + H]⁺. HRMS (TOF-MS): *m/z* calcd for C₁₇H₁₅N₂O₃ [M + H]⁺: 295.1082, found: 295.1079; IR (KBr) ν 3290, 3107, 3051, 2963, 1683, 1631, 1551, 1204, 737 cm⁻¹.

2,3,10-Trimethoxy-5,7-dihydro-6H-indolo[2,3-c]quinolin-6-one (52)

The reaction was carried out as described in general procedure D using **32** (0.060 g, 0.15 mmol, 1.0 equiv). The crude mixture was purified by flash chromatography on silica gel (eluent 9/1 CH₂Cl₂/MeOH) to afford **52** (0.031 g, 65%) as a white solid. This compound was not soluble enough to provide a correct ¹³C NMR spectrum. *R_f* = 0.4 (5% CH₃OH in CH₂Cl₂). mp 205–208 °C. ¹H NMR (DMSO-*d*₆, 400 MHz) 3.82 (s, 3H), 3.91 (s, 3H), 3.97 (s, 3H), 7.10 (s, 1H), 7.13 (s, 1H), 7.51 (s, 1H), 7.72 (d, *J* = 12.4 Hz, 2H), 11.57 (s, 1H), 12.01 (s, 1H); ESI-MS *m/z* 325 [M + H]⁺. HRMS (TOF-MS): *m/z* calcd for C₁₈H₁₆N₂O₄ [M + H]⁺: 325.1188, found: 325.1182. IR (KBr) ν 3259, 3161, 3024, 2982, 2920, 1667, 1621, 1575, 1234, 1205, 1102, 747 cm⁻¹.

10-Methoxy-2-(trifluoromethyl)-5,7-dihydro-6H-indolo[2,3-c]quinolin-6-one (53)

The reaction was carried out as described in general procedure D using **33** (0.050 g, 0.122 mmol, 1.0 equiv.). The crude mixture was purified by flash chromatography on silica gel (eluent 9/1 CH₂Cl₂/MeOH) to afford **53** (0.031 g, 75%) as a white solid. *R_f* = 0.4 (5% CH₃OH in CH₂Cl₂). mp 241–244 °C. ¹H NMR (DMSO-*d*₆, 400 MHz) 3.93 (s, 3H), 7.20 (dd, *J* = 2.0 Hz, 8.8 Hz, 1H), 7.59 (d, *J* = 8.8 Hz, 1H), 7.66 (d, *J* = 8.8 Hz, 1H), 7.75 (d, *J* = 2.0 Hz, 1H), 8.52 (s, 1H), 12.15 (s, 1H), 12.44 (s, 1H). ¹³C NMR (DMSO-*d*₆, 125 MHz) 56.1, 103.8, 114.6, 117.0, 117.2, 117.3, 118.5, 119.8, 119.8, 122.6, 122.9, 123.2, 128.9, 134.5, 137.7, 155.1, 156.2. ESI-MS *m/z* 333 [M + H]⁺. HRMS (TOF-MS): *m/z* calcd for C₁₇H₁₂N₂O₂F₃ [M + H]⁺: 333.0851, found: 333.0841; IR (KBr) ν 3235, 3153, 3060, 2951, 1658, 1610, 1574, 1210, 1030, 744 cm⁻¹.

3-Hydroxy-10-methoxy-5,7-dihydro-6H-indolo[2,3-c]quinolin-6-one (54)

The reaction was carried out as described in general procedure D using **34** (0.040 g, 0.112 mmol, 1.0 equiv.). The crude mixture was purified by flash chromatography on silica gel (eluent 9/1 CH₂Cl₂/MeOH) to afford **54** (0.023 g, 73%) as a white solid. *R_f* = 0.4 (5% CH₃OH in CH₂Cl₂). mp 227–230 °C. ¹H NMR (DMSO-*d*₆, 400 MHz) 3.92 (s, 3H), 6.82 (d, *J* = 8.4 Hz, 1H), 6.91 (d, *J* = 1.2 Hz, 1H), 7.10 (d, *J* = 8.8 Hz, 1H), 7.49 (d, *J* = 8.8 Hz, 1H), 7.76 (s, 1H), 8.24 (d, *J* = 8.4 Hz, 1H), 9.67 (s, br, 1H), 11.59 (s, 1H), 11.95 (s, 1H). ¹³C NMR (DMSO-*d*₆, 125 MHz) 56.1, 102.0, 103.7, 111.3, 111.9, 114.2, 116.9, 119.1, 122.4, 124.5, 126.6, 134.5, 136.8, 154.5, 156.2, 156.5; ESI-MS *m/z* 281 [M + H]⁺. HRMS (TOF-MS): *m/z* calcd for C₁₆H₁₃N₂O₃ [M + H]⁺: 281.0926, found: 281.0920. IR (KBr) ν 3450, 3250, 3141, 3020, 2983, 1643, 1620, 1594, 1223, 1150, 724 cm⁻¹.

2-Hydroxy-10-methoxy-5,7-dihydro-6H-indolo[2,3-c]quinolin-6-one (55)

The reaction was carried out as described in general procedure D using **35** (0.040 g, 0.112 mmol, 1.0 equiv.). The crude mixture was purified by flash chromatography on silica gel (eluent 9/1 CH₂Cl₂/MeOH) to afford **55** (0.025 g, 78%) as a white solid. *R_f* = 0.4 (5% CH₃OH in CH₂Cl₂). mp 202–205 °C. ¹H NMR (DMSO-*d*₆, 400 MHz) 3.93 (s, 3H), 6.87 (s, 1H), 7.14 (s, 1H), 7.32 (s, 1H), 7.53 (s, 1H), 7.68–7.74 (m, 2H), 9.38 (s, br 1H), 11.59 (s, 1H), 12.16 (s, 1H). ¹³C NMR (DMSO-*d*₆, 125 MHz) 56.0, 103.4, 107.8, 114.4, 114.8, 116.5, 117.5, 117.9, 119.4, 122.9, 128.3, 128.7, 134.4, 153.1, 154.7, 155.6. ESI-MS *m/z* 281 [M + H]⁺; HRMS (TOF-MS): *m/z* calcd for C₁₆H₁₃N₂O₃ [M + H]⁺: 281.0926, found: 281.0918; IR (KBr) ν 3435, 3245, 3150, 3010, 2951, 1653, 1610, 1574, 1220, 1130, 1006, 734 cm⁻¹.

2-Amino-10-methoxy-5,7-dihydro-6H-indolo[2,3-c]quinolin-6-one (56)

The reaction was carried out as described in general procedure D using **36** (0.040 g, 0.112 mmol, 1.0 equiv.). The crude mixture was purified by flash chromatography on silica gel (eluent 9/1 CH₂Cl₂/MeOH) to afford **56** (0.022 g, 70%) as a white solid. *R_f* = 0.3 (5% CH₃OH in CH₂Cl₂). mp >250 °C. ¹H NMR (DMSO-*d*₆, 400 MHz) 2.12 (s, 2H), 3.92 (s, 3H), 7.16 (dd, *J* = 1.6 Hz, 8.8 Hz, 1H), 7.40 (d, *J* = 8.8 Hz, 1H), 7.56–7.59 (m, 2H), 7.75 (d, *J* = 1.6 Hz, 1H), 8.77 (d, *J* = 1.6 Hz, 1H), 10.10 (s, 1H), 11.73 (s, 1H), 12.19 (s, 1H). ¹³C NMR (DMSO-*d*₆, 125 MHz) 56.4, 103.9, 112.4, 114.3, 116.2, 116.4, 116.5, 118.0, 118.5, 122.8, 128.7, 130.9, 134.5, 134.8, 154.8, 155.9. ESI-MS *m/z* 280 [M + H]⁺. HRMS (TOF-MS): *m/z* calcd for C₁₆H₁₃N₃O₂ [M]⁺: 279.1008, found: 279.0929. IR (KBr) ν 3285, 3157, 2993, 2957, 2930, 1675, 1628, 1410, 1147, 746 cm⁻¹.

N-(10-Methoxy-6-oxo-6,7-dihydro-5H-indolo[2,3-c]quinolin-2-yl)acetamide (57)

The reaction was carried out as described in general procedure D using **37** (0.060 g, 0.151 mmol, 1.0 equiv.). The crude mixture was purified by flash chromatography on silica gel (eluent 9/1 CH₂Cl₂/MeOH) to afford **57** (0.033 g, 69%) as a white solid. *R_f* = 0.4 (5% CH₃OH in CH₂Cl₂). mp 242–245 °C. ¹H NMR (DMSO-*d*₆, 400 MHz) 2.11 (s, 3H), 3.91 (s, 3H), 7.16 (d, *J* = 7.6 Hz, 1H), 7.38 (d, *J* = 8.8 Hz, 1H), 7.53–7.57 (t, *J* = 8.8 Hz, 2H), 7.75 (s, 1H), 8.76 (s, 1H), 10.05 (s, 1H), 11.69 (s, 1H), 12.17 (s, 1H). ¹³C NMR (DMSO-*d*₆, 125 MHz) 24.6, 56.1, 103.9, 112.4, 114.4, 116.3, 116.5, 117.7, 118.0, 118.5, 122.8, 128.7, 131.0, 134.5, 134.8, 154.8, 155.8; ESI-MS *m/z* 322 [M + H]⁺. HRMS (TOF-MS): *m/z* calcd for C₁₈H₁₆N₃O₃ [M + H]⁺: 322.1192, found: 322.1183. IR (KBr) ν 3284, 3157, 3088, 2992, 2929, 1674, 1628, 1574, 1254, 1110, 754 cm⁻¹.

9-Methoxy-5,7-dihydro-6H-indolo[2,3-c]quinolin-6-one (58)

The reaction was carried out as described in general procedure D using **38** (0.050 g, 0.147 mmol, 1.0 equiv.). The crude mixture was purified by flash chromatography on silica gel (eluent 9/1 CH₂Cl₂/MeOH) to afford **58** (0.028 g, 72%) as a white solid. *R_f* = 0.5 (5% CH₃OH in CH₂Cl₂). mp 235–237 °C. ¹H NMR (DMSO-*d*₆, 400 MHz) 3.85 (s, 3H), 6.93 (dd, *J* = 1.6 Hz, 8.8 Hz, 1H), 7.05 (d, *J* = 1.6 Hz, 1H), 7.30 (t, *J* = 7.2 Hz, 8.0 Hz, 1H), 7.39 (t, *J* = 7.2 Hz, 8.4 Hz, 1H), 7.48 (d, *J* = 8.4 Hz, 1H), 8.32 (d, *J* = 8.8 Hz, 1H), 8.37 (d, *J* = 8.0 Hz, 1H), 11.75 (s, 1H), 12.17 (s, 1H). ¹³C NMR (DMSO-*d*₆, 125 MHz) 55.4, 95.2, 95.4, 111.8, 112.1, 116.8, 118.2, 119.2, 122.5, 123.6, 126.5, 127.3, 135.5, 140.7, 155.9, 158.9. ESI-MS *m/z* 265 [M + H]⁺. HRMS (TOF-MS): *m/z* calcd for C₁₆H₁₃N₂O₂ [M + H]⁺: 265.0977, found: 265.0967. IR (KBr) ν 3235, 3155, 3027, 2938, 1655, 1611, 1574, 1107, 1027, 734 cm⁻¹.

2,9-Dimethoxy-5,7-dihydro-6H-indolo[2,3-c]quinolin-6-one (59)

The reaction was carried out as described in general procedure D using **39** (0.055 g, 0.148 mmol, 1.0 equiv.). The crude mixture was purified by flash chromatography on silica gel (eluent 9/1 CH₂Cl₂/MeOH) to afford **59** (0.029 g, 67%) as a white solid. *R_f* = 0.4 (5% CH₃OH in CH₂Cl₂). mp 235–237 °C. ¹H NMR (DMSO-*d*₆, 400 MHz) 3.86 (s, 3H), 3.92 (s, 3H), 6.95 (d, *J* = 8.4 Hz, 1H), 7.05 (d, *J* = 7.6 Hz, 2H), 7.42 (d, *J* = 8.8 Hz, 1H), 7.74 (s, 1H), 8.31 (d, *J* = 8.8 Hz, 1H), 11.66 (s, 1H, NH), 12.18 (s, 1H, NH). ¹³C NMR (DMSO-*d*₆, 125 MHz) 55.7, 56.0, 95.2, 105.8, 112.1, 114.7, 116.8, 117.7, 118.9, 119.0, 123.7, 127.7, 129.8, 140.7, 155.2, 155.4, 158.8. ESI-MS *m/z* 295 [M + H]⁺. HRMS (TOF-MS): *m/z* calcd for C₁₇H₁₅N₂O₃ [M + H]⁺: 295.1082, found: 295.1075. IR (KBr) ν 3304, 3125, 3050, 2941, 1645, 1634, 1582, 1204, 741 cm⁻¹.

10-Fluoro-2-methoxy-5,7-dihydro-6H-indolo[2,3-c]quinolin-6-one (60)

The reaction was carried out as described in general procedure D using **40** (0.060 g, 0.167 mmol, 1.0 equiv.). The crude mixture was purified by flash chromatography on silica gel (eluent 9/1 CH₂Cl₂/MeOH) to afford **60** (0.038 g, 80%) as a white solid. *R_f* = 0.5 (5% CH₃OH in CH₂Cl₂). mp 135–136 °C. ¹H NMR (DMSO-*d*₆, 400 MHz) 3.95 (s, 3H), 7.07 (s, 1H), 7.36–7.45 (m, 2H), 7.64 (s, 1H), 7.73 (s, 1H), 8.25 (d, *J* = 7.2, 1H), 11.79 (s, 1H), 12.46 (s, 1H). ¹³C NMR (DMSO-*d*₆, 125 MHz) 56.1, 106.0, 107.6, 114.6, 114.7, 117.8, 118.9, 129.4, 129.9, 135.9, 155.4, 155.5. ESI-MS *m/z* 283 [M + H]⁺. HRMS (TOF-MS): *m/z* calcd for C₁₆H₁₂N₂O₂F [M + H]⁺: 283.0882, found: 283.0873. IR (KBr) ν 3303, 3126, 3034, 2953, 2890, 1663, 1621, 1564, 1254, 1154, 1006, 745 cm⁻¹.

10-Fluoro-2-Hydroxy-5,7-dihydro-6H-indolo [2,3-c]quinolin-6-one (61)

The reaction was carried out as described in general procedure D using **41** (0.050 g, 0.145 mmol, 1.0 equiv.). The crude mixture was purified by flash chromatography on silica gel (eluent 9/1 CH₂Cl₂/MeOH) to afford **61** (0.031 g, 79%) as a white solid. *R_f* = 0.4 (5% CH₃OH in CH₂Cl₂). mp 240–243 °C. ¹H NMR (DMSO-*d*₆, 400 MHz) 6.90 (d, *J* = 8.4 Hz, 1H), 7.34–7.38 (m, 2H), 7.63–7.67 (m, 1H), 7.71 (s, 1H), 8.0 (d, *J* = 9.2, 1H), 9.35 (s, br, 1H), 11.7 (s, 1H), 12.42 (s, 1H). ¹³C NMR (DMSO-*d*₆, 125 MHz) 106.8, 107.0, 107.8, 114.5, 114.7, 114.8, 114.9, 115.3, 117.7, 118.9, 128.4, 129.8, 135.9, 153.3, 155.5. ESI-MS *m/z* 269 [M + H]⁺. HRMS (TOF-MS): *m/z* calcd for C₁₅H₁₀N₂O₂F [M + H]⁺: 269.0726, found: 269.0721. IR (KBr) ν 3410, 3247, 3150, 3014, 2997, 2920, 1645, 1607, 1514, 1254, 1104, 732 cm⁻¹.

2-Hydroxy-10-methoxy-7-methyl-5,7-dihydro-6H-indolo[2,3-c]quinolin-6-one (62)

The reaction was carried out as described in general procedure D using **42** (0.060 g, 0.162 mmol, 1.0 equiv.). The crude mixture was purified by flash chromatography on silica gel (eluent 9/1 CH₂Cl₂/MeOH) to afford **62** (0.037 g, 77%) as a white solid. *R_f* = 0.4 (5% CH₃OH in CH₂Cl₂). mp >250 °C. ¹H NMR (DMSO-*d*₆, 400 MHz) 3.92 (s, 3H), 4.27 (s, 3H), 6.84 (s, 1H), 7.27 (d, *J* = 7.6 Hz, 1H), 7.65–7.73 (m, *J* = 7.6 Hz, 3H), 9.35 (s, br, 1H), 11.57 (s, 1H). ¹³C NMR (DMSO-*d*₆, 125 MHz) 31.7, 56.1, 103.6, 107.7, 112.5, 115.0, 116.6, 117.3, 118.1, 119.2, 121.8, 127.1, 128.3, 135.8, 153.1, 155.0, 156.3. ESI-MS *m/z* 295 [M + H]⁺. HRMS (TOF-MS): *m/z* calcd for C₁₇H₁₅N₂O₃ [M + H]⁺: 295.1082 found: 295.1072. IR (KBr) ν 3450, 3180, 3070, 2954, 1661, 1651, 1517, 1210, 1105, 1070, 739 cm⁻¹.

10-Methoxy-7-methyl-2-(trifluoromethyl)-5,7-dihydro-6H-indolo[2,3-c]quinolin-6-one (63)

The reaction was carried out as described in general procedure D using **43** (0.055 g, 0.130 mmol, 1.0 equiv.) The crude mixture was purified by flash chromatography on silica gel (eluent 9/1 CH₂Cl₂/MeOH) to afford **63** (0.038 g, 84%) as a white solid. *R*_f = 0.7 (5% CH₃OH in DCM). mp >250 °C. ¹H NMR (DMSO-*d*₆, 400 MHz) 3.94 (s, 3H), 4.30 (s, 3H), 7.27 (d, *J* = 8.8 Hz, 1H), 7.61 (d, *J* = 8.4 Hz, 1H), 7.69–7.73 (m, *J* = 7.6 Hz, 8.4 Hz, 3H), 8.47 (s, 1H), 12.12 (s, 1H); ¹³C NMR (DMSO-*d*₆, 125 MHz) 31.8, 56.1, 103.7, 112.8, 116.9, 117.1, 117.4, 118.2, 119.6, 121.5, 122.6, 125.1, 127.2, 135.9, 137.6, 155.4, 156.8. ESI-MS: *m/z* 347 [M + H]⁺. HRMS (TOF-MS): *m/z* calcd for C₁₈H₁₄N₂O₂F₃ [M + H]⁺: 347.1007, found: 347.1001. IR (KBr) ν 3110, 3010, 2951, 2910, 1657, 1594, 1200, 1130, 1010, 744 cm⁻¹.

2-(Dimethylamino)-10-methoxy-7-methyl-5,7-dihydro-6H-indolo[2,3-c]quinolin-6-one (64)

The reaction was carried out as described in general procedure D using **44** (0.065 g, 0.163 mmol, 1.0 equiv.). The crude mixture was purified by flash chromatography on silica gel (eluent 9/1 CH₂Cl₂/MeOH) to afford **64** (0.039 g, 75%) as a white solid. *R*_f = 0.7 (5% CH₃OH in DCM). mp 231–234 °C. ¹H NMR (DMSO-*d*₆, 400 MHz) 3.00 (s, 6H), 3.91 (s, 3H), 4.28 (s, 3H), 6.94 (dd, *J* = 2.4 Hz, 8.8 Hz, 1H), 7.21 (dd, *J* = 9.2 Hz, 2.4 Hz, 1H), 7.31 (d, *J* = 9.2 Hz, 1H), 7.44 (d, *J* = 2.4 Hz, 1H), 7.65 (d, *J* = 8.8 Hz, 1H), 7.16 (d, *J* = 2.4 Hz, 1H), 11.51 (s, 1H). ¹³C NMR (DMSO-*d*₆, 125 MHz) 31.7, 41.2, 55.9, 103.9, 104.9, 112.4, 113.6, 116.2, 116.9, 118.3, 119.2, 121.9, 126.9, 127.3, 135.9, 146.9, 154.8, 156.1; ESI-MS: *m/z* 322 [M + H]⁺. HRMS (TOF-MS): *m/z* calcd for C₁₉H₂₀N₃O₂ [M + H]⁺: 322.1556, found: 322.1555. IR (KBr) ν 3145, 3020, 2950, 2910, 1675, 1600, 1564, 1210, 754 cm⁻¹.

Cell culture

HCT116 cells were cultured in McCoy's medium. SH-SY5Y, MDA-MB231 and U-2 OS cells were cultured in Dulbecco's modified Eagle's medium (DMEM) and hTERT RPE-1 cells in DMEM:F12 medium. All media were supplemented with 10% foetal calf serum and cells were cultured at 37 °C in a 5% CO₂ humidified atmosphere.

Cell viability

Cells were grown in 96-well plates in the presence of a fixed concentration of 25 μ M of each compound (for cell viability primary assessment) or increasing concentrations of each compound (from 50 to 0.05 μ M) for 48 h (for EC₅₀ determination). Cell viability was then assessed using the CellTiter96 AQueous cell proliferation assay from Promega according to the manufacturer's instructions. Each experiment was done in triplicate and EC₅₀ were determined from the dose-response curves according to the signal given by the control (0.1% DMSO) set at 100% viability using Prism GraphPad software.

3D Spheroid viability

U-2 OS cells were seeded at 5000 cells per well and HCT116 at 1500 cells per well, in 96-well black ULA plates (Ultra Low Adherence, Corning). After centrifugation at 200 *g* for 10 min, spheroids were incubated at 37 °C for 3 days in order to reach 400 μ m in diameter. Compounds were then added at a single dose (2.5, 5, or 10 μ M) and cell viability was measured after 7 days

using the CellTiter-Glo® 3D Cell Viability Assay (Promega) following the manufacturer's protocol. Luminescence was measured using an EnVision® plate reader (Perkin Elmer).

Endogenous haspin activity measurement

U-2 OS cells were grown on glass coverslips, treated for 16 h then fixed with 4% paraformaldehyde in PBS, permeabilized by 0.15% Triton-X100 for 2 min, blocked for 15 min in 4% BSA in PBS and processed using standard immunofluorescence protocols. Primary antibodies included anti-phospho-Thr3 Histone H3 (1/1000 dilution, Millipore) and anti- α -tubulin (1/5000 dilution, clone B512, Sigma). Images were acquired with a Coolsnap HQ2 CCD camera (Photometrics) on a Zeiss Axio microscope (Carl Zeiss) using a 63x NA 1.40 objective. Image acquisition and processing were performed using Metamorph (Molecular Device). Quantification of signal intensity was performed using ImageJ software (NIH).

Cell cycle analysis

After treatment with the compounds, cells were trypsinized and washed once in PBS. Cells were fixed for 1 h in ice-cold 70% ethanol, then washed once in PBS, centrifuged at 200 *g* and resuspended in a PBS buffer containing 100 μ g/ml RNase A (Thermo Scientific) and 40 μ g/ml propidium iodide (Life Technologies). DNA content was determined using a flow cytometer Attune™ NxT (ThermoFisher) and ten thousand events were collected in each run. The data were analysed using FCS Express 7 Pro software (De Novo).

Kinase assays

Kinase activities were determined using the ADP-Glo methodology (ADP-Glo Kinase Assay; Promega) according to the assay described by Nguyen et al.³² except for MmCLK1. The later was assayed in the following buffer: 10 mM MgCl₂, 1 mM EGTA, 1 mM DTT, 25 mM Tris-HCl pH 7.5, 50 μ g/ml heparin, 0.15 mg/ml BSA, with 0.027 μ g/ μ l of the following peptide: GRSRSRSRSRSR as substrate.

Molecular modelling

Structure preparation

Marvin was used for drawing chemical structures³³. Structures were prepared with VSPrep, a workflow dedicated to the preparation of ligands for virtual screening³⁴, and finally given as input to Glide, the docking software from the Schrödinger Molecular Modelling Suite 2019-01³¹. Structural data of CLK1 kinase complexed with a methyl 9-anilinothiazolo[5,4-*f*]quinazoline-2-carbimide (EHT1610) compound were retrieved from the protein data bank³⁵, PDB entry 6YTI (unpublished data). DYRK1A in complex with a pyrido[2,3-*d*]pyrimidine inhibitor, the *N*-(5-(((1*R*)-3-amino-1-(3-chlorophenyl)propyl)carbamoyl)-2-chlorophenyl)-2-methoxy-7-oxo-7,8-dihydropyrido[2,3-*d*]pyrimidine-6-carboxamide, was retrieved from the protein data bank³⁵, PDB entry 4MQ1³⁶. Structural data of Haspin kinase complexed with an imidazo[1,2-*b*]pyridazine derivative compound were retrieved from the protein data bank³⁵, PDB entry 3F2N (unpublished data). The three high-resolution crystal structures of CLK1, DYRK1A and Haspin were superimposed before carrying out molecular docking experiments. All the receptors were prepared using the Protein Preparation Wizard workflow from the Schrödinger Molecular Modelling Suite

2019–01. Hydrogen atoms were added, water molecules were removed, the hydrogen network automatically was optimised and finally proteins were minimised (OLPS2005 force field) with a convergence criterion of RMSD on heavy atoms of 0.3 Å (other parameters were fixed to their default values).

Docking parameters

Docking grids were centred and sized on crystalised ligands. Docking calculations were performed with extra precision. Ligand flexibility was considered and the option of sampling of ring conformation was activated. A maximum of 100 poses were generated and a post-docking minimisation was performed.

Conclusion

We have synthesised a series of new Lamellarin analogues using the indolo[2,3-*c*]quinolone-6-one core. The analogues were obtained after a sequence involving (i) a palladium catalysed cross coupling reaction between 2-indolic esters and 2-nitrophenyl boronic acids as building blocks, and (ii) a cyclic lactam formation involving a reduction and an annelation. Twenty-two novel derivatives were synthesised and evaluated for their inhibitory activity on Haspin kinase and on a panel of 7 other protein kinases for selectivity assessment. Among this series, 8 compounds inhibited Haspin kinase with IC_{50} below 10 nM. Docking studies showed a double hydrogen bond between the lactam and the hinge region of the kinase. The most active compounds **49** and **55** possess IC_{50} of 1 and 2 nM respectively with selectivity towards the parent kinases DYRK1A and CLK1 between a 13 and 65-fold factor. Furthermore, the most selective compound **55** exerted an interesting cellular effect on the osteosarcoma U-2 OS cell line as well as on U-2 OS and colorectal carcinoma HTC116 spheroid viability. Additionally, we further validated the functionality of compound **55** on endogenous Haspin activity in cells. This interesting Haspin inhibitor will be used in further studies to develop efficient and selective Haspin inhibitors.

Acknowledgements

The authors thank Gaëlle Al Feghali for technical assistance on FACS data analysis. The authors wish to thank the Cancéropôle Grand Ouest "Marine Molecules, Metabolism and Cancer network", IBI SA (French Infrastructure en sciences du vivant: biologie, santé et agronomie), Biogenouest (Western France life science and environment core facility network supported by the Conseil Régional de Bretagne) for supporting KISSf facility.

Author contributions

Conceptualization, S.Ro. and C.N.; Methodology chemistry, S.A., S.Ro. and C.N.; Methodology biology, S.Br., S.Ba. and S.Ru.; Molecular modeling, S.Bo. and P.B.; Investigation, S.A., L.X., P. X., M.T., B.J., S.Bo., S.Ba., P.B., F.B., S.Ru., S.Ro. and C. N.; Writing –Original Draft, S.Ru., S.Ro., and C.N.; Writing–Review & Editing, S.Ru., S.Ro. S.Bo., S.A., P.B., F.B. and C.N.; Funding Acquisition & Resources & Supervision, S.Ru., S.Ro and C.N.

Disclosure statement

No potential conflict of interest was reported by the author(s). This work was conducted in the absence of any commercial or

financial relationships that could be construed as a potential conflict of interest.

Funding

This work was funded by "La Ligue contre le Cancer du Grand Ouest" committee (districts 29, 22, 56, 35, 45 and 79) in Région Centre Val de Loire, by the RTR Motivhealth. This research was supported by the Drug Discovery Pipeline of Guangzhou Institute of Biomedicine and Health, GIBH.

References

1. Jiménez C. Marine natural products in medicinal chemistry. *ACS Med Chem Lett* 2018;9:1632–61.
2. Bharate SB, Sawant SD, Singh PP, Vishwakarma RA. Kinase inhibitors of marine origin. *Chem Rev* 2013;113:6761–815.
3. Marston A. Natural products as a source of protein kinase activators and inhibitors. *Curr Top Med Chem* 2011;11:1333–9.
4. Nakano H, Omura S. Chemical biology of natural indolocarbazole products: 30 years since the discovery of staurosporine. *J Antibiot* 2009;62:17–26.
5. Knapper S, Burnett AK, Littlewood T, et al. A phase 2 trial of the FLT3 inhibitor lestaurtinib (CEP701) as first-line treatment for older patients with acute myeloid leukemia not considered fit for intensive chemotherapy. *Blood* 2006;108:3262–70.
6. Hexner EO, Serdikoff C, Jan M, et al. Lestaurtinib (CEP701) is a JAK2 inhibitor that suppresses JAK2/STAT5 signaling and the proliferation of primary erythroid cells from patients with myeloproliferative disorders. *Blood* 2008;111:5663–71.
7. Wick W, Puduvalli VK, Chamberlain MC, et al. Phase III study of enzastaurin compared with lomustine in the treatment of recurrent intracranial glioblastoma. *J Clin Oncol* 2010;28:1168–74.
8. Routier S, Coudert G, Mérour J-Y. Synthesis of naphthopyrrolo[3,4-*c*]carbazoles. *Tetrahedron Lett* 2001;42:7025–8.
9. Bourderioux A, Kassis P, Mérour J-Y, Routier S. Synthesis of new fused and substituted benzo and pyrido carbazoles via C-2 (het)arylindoles. *Tetrahedron* 2008;64:11012–9.
10. Lefoix M, Coudert G, Routier S, et al. Novel 5-azaindolocarbazoles as cytotoxic agents and Chk1 inhibitors. *Bioorg Med Chem* 2008;16:5303–21.
11. Routier S, Mérour J-Y, Dias N, et al. Synthesis and biological evaluation of novel phenylcarbazoles as potential anticancer agents. *J Med Chem* 2006;49:789–99.
12. Routier S, Peixoto P, Mérour JY, et al. Synthesis and biological evaluation of novel naphthocarbazoles as potential anticancer agents. *J Med Chem* 2005;48:1401–13.
13. Bourderioux A, Routier S, Bénateau V, Mérour J-Y. Synthesis of benzo analogs of oxoarcyriaflavins and caulersine. *Tetrahedron* 2007;63:9465–75.
14. Bourderioux A, Bénateau V, Mérour J-Y, et al. Synthesis and biological evaluation of novel oxophenylarcyriaflavins as potential anticancer agents. *Org Biomol Chem* 2008;6:2108–17.
15. Neagoie C, Vedrenne E, Buron F, et al. Synthesis of chromeno[3,4-*b*]indoles as Lamellarin D analogues: A novel DYRK1A inhibitor class. *Eur J Med Chem* 2012;49:379–96.

16. Fan H, Peng J, Hamann MT, Hu J-F. Lamellarins and related pyrrole-derived alkaloids from marine organisms. *Chem Rev* 2008;108:264–87.
17. Youssef DTA, Almagthali H, Shaala LA, Schmidt EW. Secondary metabolites of the genus *didemnum*: a comprehensive review of chemical diversity and pharmacological properties. *Mar Drugs* 2020;18:307.
18. Baunbaek D, Trinkler N, Ferandin Y, et al. Anticancer alkaloid lamellarins inhibit protein kinases. *Mar Drugs* 2008;6:514–27.
19. Zhang T-Y, Liu C, Chen C, et al. Copper-mediated cascade C-H/N-H annulation of indolocarboxamides with arynes: construction of tetracyclic indoloquinoline alkaloids. *Org Lett* 2018;20:220–3.
20. Li Z, Wang W, Zhang X, et al. One-pot synthesis of indolo[2,3-c]quinolin-6-ones by sequential photocyclizations of 3-(2-Azidophenyl)-N-phenylacrylamides. *Synlett* 2012;24:73–8.
21. Szabó T, Papp M, Németh DR, et al. Synthesis of indolo[2,3-c]quinolin-6(7H)-ones and antimalarial Isonocryptolepine. Computational study on the Pd-catalyzed intramolecular C–H arylation. *J. Org. Chem* 2021;86:128–45.
22. Gu C-X, Chen W-W, Xu B, Xu M-H. Synthesis of indolo[2,3-c]coumarins and indolo[2,3-c]quinolinones via microwave-assisted base-free intramolecular cross dehydrogenative coupling. *Tetrahedron* 2019;75:1605–11.
23. Chen Z, Wang X. A Pd-catalyzed, boron ester-mediated, reductive cross-coupling of two aryl halides to synthesize tricyclic biaryls. *Org Biomol Chem* 2017;15:5790–6.
24. Sakamoto T, Nagano T, Kondo Y, Yamanaka H. Palladium-catalyzed coupling reaction of 3-iodoindoles and 3-iodobenzothienophene with terminal acetylenes. *Chem Pharm Bull* 1988;36:2248–52.
25. Collibee SE, Yu J. A facile and convenient synthesis of functionalized ortho-nitrophenylboronic acids. *Tetrahedron Lett* 2005;46:4453–5.
26. Elie J, Feizbakhsh O, Desban N, et al. Design of new disubstituted imidazo[1,2-b]pyridazine derivatives as selective Haspin inhibitors. Synthesis, binding mode and anticancer biological evaluation. *J Enzyme Inhib. Med. Chem* 2020;35:1840–53.
27. Feizbakhsh O, Place M, Fant X, et al. The mitotic protein kinase haspin and its inhibitors. In: Prignet C, ed. *Protein phosphorylation*. Ch. 02. Rijeka: InTech; 2017.
28. Friesner RA, Murphy RB, Repasky MP, et al. Extra precision glide: docking and scoring incorporating a model of hydrophobic enclosure for protein-ligand complexes. *J. Med. Chem* 2006;49:6177–96.
29. Halgren TA, Murphy RB, Friesner RA, et al. Glide: a new approach for rapid, accurate docking and scoring. 2. Enrichment factors in database screening. *J Med Chem* 2004;47:1750–9.
30. Friesner RA, Banks JL, Murphy RB, et al. Glide: a new approach for rapid, accurate docking and scoring. 1. Method and assessment of docking accuracy. *J Med Chem* 2004;47:1739–49.
31. Schrödinger release 2019-1: Glide. New York, NY: Schrödinger, LLC; 2020.
32. Nguyen T-N-D, Feizbakhsh O, Sfecci E, et al. Kinase-based screening of marine natural extracts leads to the identification of a cytotoxic high molecular weight metabolite from the Mediterranean Sponge *Crambe tailliezi*. *Mar. Drugs* 2019;17:569.
33. Marvin 20.13.10, 2020 ChemAxon. <http://www.chemaxon.com>.
34. Gally JM, Bourg S, Fogha J, et al. VSPrep: A KNIME workflow for the preparation of molecular databases for virtual screening. *Curr Med Chem* 2019;27:6480–6494.
35. Berman HM, Westbrook J, Feng Z, et al. The protein data bank. *Nucleic Acids Res* 2000;28:235–42.
36. Anderson K, Chen Y, Chen Z, et al. Pyrido[2,3-d]pyrimidines: discovery and preliminary SAR of a novel series of DYRK1B and DYRK1A inhibitors. *Bioorg Med Chem Lett* 2013;23:6610–5.